On the modeling of waste deposition around deep aquaculture sites in Newfoundland

Andry W Ratsimandresy, Dounia Hamoutene, Brent Law, Vanessa Oldford, Flora Salvo, Aaron Bennett

Fisheries and Oceans Canada
Northwest Atlantic Fisheries Center
St. John's, NL, A1C 5X1
Canada

2026

Canadian Technical Report of
Fisheries and Aquatic Sciences 3745

Fisheries and Oceans Canada | Pêches et Océans Canada

Canada

Canadian Technical Report of Fisheries and Aquatic Sciences

Technical reports contain scientific and technical information that contributes to existing knowledge but which is not normally appropriate for primary literature. Technical reports are directed primarily toward a worldwide audience and have an international distribution. No restriction is placed on subject matter and the series reflects the broad interests and policies of Fisheries and Oceans Canada, namely, fisheries and aquatic sciences.

Technical reports may be cited as full publications. The correct citation appears above the abstract of each report. Each report is abstracted in the data base *Aquatic Sciences and Fisheries Abstracts*.

Technical reports are produced regionally but are numbered nationally. Requests for individual reports will be filled by the issuing establishment listed on the front cover and title page.

Numbers 1-456 in this series were issued as Technical Reports of the Fisheries Research Board of Canada. Numbers 457-714 were issued as Department of the Environment, Fisheries and Marine Service, Research and Development Directorate Technical Reports. Numbers 715-924 were issued as Department of Fisheries and Environment, Fisheries and Marine Service Technical Reports. The current series name was changed with report number 925.

Rapport technique canadien des sciences halieutiques et aquatiques

Les rapports techniques contiennent des renseignements scientifiques et techniques qui constituent une contribution aux connaissances actuelles, mais qui ne sont pas normalement appropriés pour la publication dans un journal scientifique. Les rapports techniques sont destinés essentiellement à un public international et ils sont distribués à cet échelon. II n'y a aucune restriction quant au sujet; de fait, la série reflète la vaste gamme des intérêts et des politiques de Pêches et Océans Canada, c'est-à-dire les sciences halieutiques et aquatiques.

Les rapports techniques peuvent être cités comme des publications à part entière. Le titre exact figure au-dessus du résumé de chaque rapport. Les rapports techniques sont résumés dans la base de données *Résumés des sciences aquatiques et halieutiques.*

Les rapports techniques sont produits à l'échelon régional, mais numérotés à l'échelon national. Les demandes de rapports seront satisfaites par l'établissement auteur dont le nom figure sur la couverture et la page du titre.

Les numéros 1 à 456 de cette série ont été publiés à titre de Rapports techniques de l'Office des recherches sur les pêcheries du Canada. Les numéros 457 à 714 sont parus à titre de Rapports techniques de la Direction générale de la recherche et du développement, Service des pêches et de la mer, ministère de l'Environnement. Les numéros 715 à 924 ont été publiés à titre de Rapports techniques du Service des pêches et de la mer, ministère des Pêches et de l'Environnement. Le nom actuel de la série a été établi lors de la parution du numéro 925.

Canadian Technical Report of
Fisheries and Aquatic Sciences 3745

2026

On the modeling of waste deposition around deep aquaculture sites in Newfoundland

by

Andry W Ratsimandresy*[1], Dounia Hamoutene*[2], Brent Law*[3], Vanessa Oldford*[1], Flora Salvo[+], Aaron Bennett[++]

*Fisheries and Oceans Canada
[1]Northwest Atlantic Fisheries Centre
St. John's, NL, A1C 5X1
Canada

*Fisheries and Oceans Canada
[2]St. Andrews Biological Station
St. Andrews, NB, E5B 0E4
Canada

*Fisheries and Oceans Canada
[3]Bedford Institute of Oceanography
Dartmouth, NS, B2Y 4A2
Canada

[+]Merinov
96 montée de Sandy beach
Gaspé, QC, G4X 2V6
Canada

[++]MOWI Canada East Inc.

Cat. No. Fs97-6/3745E-PDF ISBN 978-0-660-97695-2 ISSN 1488-5379

https://doi.org/10.60825/6et7-jx83

Correct citation for this publication:

Ratsimandresy, A.W., Hamoutene, D., Law, B., Oldford, V., Salvo, F., Bennett, A. 2026. On the modeling of waste deposition around deep aquaculture sites in Newfoundland. Can. Tech. Rep. Fish. Aquat. Sci. 3745: viii + 37 p. https://doi.org/10.60825/6et7-jx83

Table of Contents

List of Tables

List of Figures

ABSTRACT

Ratsimandresy, A.W., Hamoutene, D., Law, B., Oldford, V., Salvo, F., Bennett, A. 2026. On the modeling of waste deposition around deep aquaculture sites in Newfoundland. Can. Tech. Rep. Fish. Aquat. Sci. 3745: viii + 37 p. https://doi.org/10.60825/6et7-jx83

Finfish aquaculture in Newfoundland includes a grow out phase in open-net cages often set up in deep fjord-like sites. With the expansion of the industry and the concern for environmental impact, two coastal steep and deep sites located in the same bay were studied in order to analyze the deposition associated with the farming activity. Ocean currents at various depths were measured for seven months at one location close to each farming site. These currents together with weekly feeding data were used to force the deposition model DEPOMOD which computed the dispersion and deposition of waste from the farms. The modeled performance was assessed by comparing computed waste deposition to direct deposition measurement obtained from programmable sediment traps and to seafloor video observations. Our analysis of the model output shows that deposition can take place at a distance greater than 500 m away from the cage array; however, the location of the deposition would vary depending on the vertical resolution of the ocean current data used to force the model, thus leading to a variation in the site footprint. Our findings show that DEPOMOD has important limitations in reproducing the observed waste deposition at the coastal deep environment where finfish farms are located in Newfoundland and in explaining the benthic survey observations. Consideration of resuspension in the model run can also generate larger footprints. For instance, in the present study, less than 2 % of the recorded current speeds were over the resuspension threshold; however, the amount of deposition happening outside of a 1000 x 1000 m^2 domain changed from 6 % to 60 % of the total expected deposition between the DEPOMOD run without resuspension and that with resuspension, neither of the case runs explained the observed deposition.

RÉSUMÉ

Ratsimandresy, A.W., Hamoutene, D., Law, B., Oldford, V., Salvo, F., Bennett, A. 2026. On the modeling of waste deposition around deep aquaculture sites in Newfoundland. Can. Tech. Rep. Fish. Aquat. Sci. 3745: viii + 37 p. https://doi.org/10.60825/6et7-jx83

Les activités de pisciculture à Terre-Neuve incluent une phase de grossissement de poissons dans des cages suspendues à enclos ouvert installées dans une région profonde aux allures de fjord. Avec l'expansion de l'activité et le souci d'impacts environnementaux, deux sites très profonds situés dans une même baie ont été étudiés dans le but de comprendre les dépôts associés à l'activité aquacole. Des mesures de courants marins à différentes profondeurs ont été effectuées à une station près de chaque site pendant une période de sept mois. Ces données de courants océaniques combinées avec des données hebdomadaires d'alimentation des poissons ont été utilisées comme forçage du modèle de déposition DEPOMOD pour calculer la dispersion et la déposition de déchets venant des fermes aquacoles. Le résultat du modèle est comparé aux observations recueillies à l'aide de collecteurs de sédiments programmables et ceux venant de la distribution de la faune benthique afin d'évaluer la performance du modèle. Notre analyse des résultats du modèle montre que les dépôts peuvent avoir lieu à une distance supérieure à 500 m du site aquacole; par contre, les lieux de déposition peuvent changer selon la résolution verticale des données de courants marins considérées comme forçages du modèle entrainant ainsi un changement de l'empreinte du site. Notre étude montre que DEPOMOD est très limité pour simuler la déposition de déchets dans les environnements côtiers profonds où les activités de pisciculture à Terre-Neuve ont lieu et pour expliquer les observations de faunes benthiques. L'inclusion du processus de resuspension dans la modélisation peut aussi générer un changement de l'empreinte de l'activité menant à une empreinte plus large. Par exemple, pour cet étude, moins de 2 % des vitesses de courant étaient au-dessus du seuil de resuspension de particules; cependant, la quantité de déposition en dehors d'un domaine de 1000 x 1000 m^2 aux alentours du site variait de 6 % à 60 % de la totalité des dépositions entre le cas de modèle sans resuspension et celui avec resuspension, aucun de ces deux cas n'explique le résultat de la mesure de déposition effectuée.

1. INTRODUCTION

Following the growth of global population and the demand for food, aquaculture has become an important global source of protein and continues to expand (FAO 2018). The rapid growth of the salmonid aquaculture industry has led to concern about the environmental benthic impacts associated with fish farm activity (Broch et al., 2017; Keeley et al., 2019; Law et al., 2014; 2019, Rector et al. 2021). These impacts are the result of waste from the farm cages sinking while dispersing within the water column and settling to the seafloor (Chamberlain and Stucchi 2007). Modelling plays a role in understanding where the waste settles to the seafloor (Cromey et al. 2002, Cromey and Black 2005, Stucchi et al. 2005, Broch et al. 2017, Hargrave et al 2022). An assessment of the performance of a model on specific conditions needs to be carried out before it can be used for any application of interest (Page et al. 2023). This includes evaluation of its behavior in the region of interest, comparison of its output with observations related to benthic impacts, and sensitivity analysis to help understand model accuracy upon changes in the input variables.

From a regulatory perspective to complete a site licensing application, an estimation of the geographic distribution of the deposition of biochemical oxygen-demanding matter (BOD) for flux values of 1, 5, and 10 g Carbon/m^2/day is required by DFO's Aquaculture Activity Regulations (AAR 2015). Furthermore, there is a need to understand how the deposition of the waste is initially distributed on the seafloor in order to quantify a relationship between benthic impacts and the deposition of waste. Deposition can be measured by using sediment sampling via grab or core samplers (e.g. Chang et al. 2014, Keeley et al. 2019) or by using sediment traps to collect settling particles (e.g. Hargrave et al. 2022, Podemski et al. 2022; amongst others). Collection of sediment samples can only be carried out at discrete locations due to the high cost (time and expense) of field work and their analysis. The other method to evaluate waste deposition is to use deposition models. Page et al. (2023) did an extensive review of the different models aiming to study deposition of aquaculture waste. Early models computed the horizontal distance travelled by waste particles before deposition, using a horizontal current speed at one point and the time necessary for a particle to reach the bottom (Silvert and Swoles 1996; Chang et al. 2012). More recent complex models made use of a coupled hydrodynamic and particle tracking model (e.g. Broch et al. 2017), the former computes the 3D field of water currents around a site and the later estimates how the waste particles move following the 3D current information, while sinking to the seafloor. DEPOMOD is one of the early models used to assess the deposition of waste associated with aquaculture activity (Cromey et al 2002). Analysis to validate whether DEPOMOD can be used to study deposition of aquaculture waste has been performed in Scotland and in several Canadian regions and for various farmed species (e.g. Cromey et al. 2002 for Scotland, Weise et al. 2009 for shellfish, Podemski et al. 2022 for freshwater aquaculture) with the general conclusion that more study is needed in order to select model parameters that lead to better simulation of the deposition and particle resuspension. In Newfoundland, finfish aquaculture can take place in different coastal conditions including narrow and deep bays (>100 m) with hard and patchy substrate, where the stratification of the water is seasonal (Donnet et al. 2022, Donnet et al. 2018a, 2018b) and where the water circulation is complex (Ratsimandresey et al. 2019); in this context, DEPOMOD needs to be further evaluated to validate prediction of waste deposition to the seafloor for regulatory compliance (DFO 2014).

In hard dominated seafloor sites, visual monitoring has been used to document changes in benthic conditions around Newfoundland finfish farms (Hamoutene et al. 2015, 2016, 2018; Salvo et al. 2017) and showed a decrease in epibenthic taxon richness after production in the near-cage area as a result of aquaculture activity. Evaluating the intensity of the effect is part of the AAR requirement (AAR 2015)

which stipulates that visual indicators of organic enrichment through video survey should not be observed in more than 70 % of the locations specified in the monitoring standard in order for restocking to be approved. In northern Norway fjord systems, Dunlop et al (2021) combined substrate and biological mapping techniques based on remote sensing and low-cost towed camera to examine the spatial patterns of benthic epifaunal community composition and spatial variation of organic enrichment around farms. They concluded that the epifaunal distribution on mixed- and hard-bottom substrates is impacted by farm-derived waste as well as by abiotic factors, such as current velocity, substrate type, and seafloor type.

The objective of the present work is to discuss the performance of the deposition model DEPOMOD to assess aquaculture waste deposition released from sites located in a deep fjord. This report is divided into various sections: the first section describes the sites of interest, the field measurements which include oceanographic data, benthic survey, and sediment collection using sediment traps, as well as the model used in the study. The second section provides the results of the measurement and the different model runs, followed by a discussion on the limitation of the use of DEPOMOD in a region with complex water circulation. Finally, a summary of the results of the study and recommendations on the characteristics of a model that would improve the analysis of waste deposition in the Newfoundland region is provided.

2. MATERIAL AND METHODS

2.1. SITE DESCRIPTION

The study was carried out in a long and narrow bay on the southern coast of Newfoundland, Canada. Within the bay, two of the leases for finfish, Chaleur Bay (Site A, 7 km from the mouth) and Friar Cove (Site B, 4.5 km from the mouth), were active. The bay is 11 km long and 1.2 km wide (at its widest part) and runs mainly south to north but with various changes in orientation (Figure 1). It is a fjord like bay with bathymetry as deep as 270 m. The Canadian Hydrographic Service; however, has a very limited bathymetry data for the area; as such, detailed bathymetry in the bay is only available within the lease areas as provided by our industry partner. The depth within the lease area at Site A ranges between 1 and 144 m while at Site B it ranges between 1 and 266 m (DFO 2022). The two sites were located over patchy substrates (hard and soft bottom) according to the information provided by the industry partner.

2.2. DATA COLLECTION

2.2.1. Oceanographic measurements

Two mooring lines containing various oceanographic instruments were placed near the aquaculture sites (one south of each site, Figure 1). The lines were moored at a distance as close as possible to the aquaculture cage arrays but far enough to avoid perturbation of the cage anchor lines onto the oceanographic data measurements. The oceanographic moorings included two (Site A) and three (Site B) Teledyne RDI Workhorse Acoustic Doppler Current Profilers (ADCP) to measure ocean currents for the whole water column. For each line, two 300 KHz ADCPs were installed at mid-depth (72 m and 99 m depth for Site A and Site B, respectively), with one ADCP looking up and the other one looking down in order to measure ocean currents over the whole water column. The third ADCP at Site B was a downward-looking 1200 KHz ADCP located relatively close to the seafloor to allow measurement of near bottom currents (at ~257 m depth). The mooring lines collected measurements for seven consecutive months from 27 February 2022 to 27 September 2022.

Vertical profiles of temperature and salinity were collected around the sites only at the time of the

mooring deployment and recovery. The measurements were carried out using a Sea-Bird Electronic (SBE) CTD model SBE25plus instrument. These profiles gave information on the water structure in winter (Feb) and fall (Sep) in the area. ADCP and CTD data were processed and quality checked as described in Donnet et al. (2020) and Donnet et al. (2018a).

2.2.2. Sediment traps

Two programmable multi-bottle sediment traps were moored directly at the edge of the cage array, one at each site, to collect near-field deposition (Figure 1). Each programmable trap was composed of 8 bottles and was programmed to collect depositing materials for a pre-determined period of time, 10 days in the present study, at specific dates as described in Table 1. Wide mouth bottles were used, each having a 0.32 m^2 opening, a 2:1 in Width:Height ratio, a sealable top to prevent spilling, and a baffled top to allow longer term collection (Law and Hill, 2019). Each bottle was filled with heavy salt water (50 ppm) and 10 % formaldehyde to both prevent spilling of particulate material once trapped in the bottle and to fix samples to prevent biological growth. The sediment traps were deployed during the same period as the oceanographic moorings.

The total flux measured by the trap was computed by dividing the weight of the dry material of the collected suspended particulate material by the area of the opening of the trap, 0.32 m^2, and by the number of days the bottle was open for collection. The dry material was obtained from filtering a known volume of suspended particulate material collected in each of the bottles of the sediment trap and drying the filter at approximately 60°C for 24 hours. Glass fiber filters (i.e. 25 mm) type D were used for all flux calculations. Three samples from each bottle were processed and used in the calculations to determine and average flux value

2.2.3. Benthic survey

Benthic video monitoring was performed at the end of production, October 2022, following the protocol established by regulatory and advisory documents (DFO 2012, Mabrouk et al. 2014). The video data is the combination of two types of monitoring, one was the AAR monitoring completed along transects extending from the cage edge at each corner of the cage array, and the second was along defined transects at some distance from the cage array (but not exceeding a couple of hundreds of meters. Each transect measured 100 m in length. Video footage was recorded using an underwater camera mounted on an aluminum frame with a 50 cm x 50 cm quadrate and coupled to a GPS recorder (at the surface). Still images were extracted from the video footage, converted into image files, and visually analyzed to identify seafloor and taxa composition (counting also the number of species/groups of fauna and flora present within the quadrate). The analysis was reported on a spreadsheet table which contains information on station name, GPS coordinates, depth, substrate type, and presence or absence of organisms. The dominant substrate types were defined as boulder, cobble, pebble, silt, and sand as described in Wentworth (1922).

As in previous video monitoring studies carried out in Newfoundland (Hamoutene et al. 2018, 2017; Salvo et al. 2018), the species or taxa were classified and grouped into high taxonomic level categories by taking into account their importance in term of feeding strategy, dependence with depth, substrata or shape. Those groups were adapted to the present study and abundance and diversity were recorded from each still image. Abundance is given by the number of observed individuals per m^2 during the survey without any distinction among species, while diversity is the number of different species/taxa/groups observed from each still image.

2.3. DEPOSITION MODELLING

DEPOMOD v2.2 (Cromey et al. 2002) was used to compute the spatial distribution of deposition in the vicinity of fish farms in Scottish fjordic systems. DEPOMOD uses site characteristics (bathymetry, cage location, husbandry information, and ocean current velocity) as input. It applies a Lagrangian method to simulate the movement of particles throughout the water column as they are released from an active aquaculture farm. The model has also been used in the study of benthic impact at salmon farms in British Columbia, Canada (Chamberlain et al. 2005, Chamberlain and Stucchi 2007) and New Zealand (Keeley et al. 2013). It consists of three modules.

The first module is the grid generation which is used to define the geographic domain where deposition is computed. The size of the grid cells, the location of each cell, the depth which corresponds to the center of the cells, and the total number of cells are specified in this module. DEPOMOD requires the definition of a fine scale minor grid in the immediate vicinity of the cage area and a larger scale major grid for areas further away. In the present analysis, these two grids had the same resolution with the major grid being 99 x 99 cells and the minor one 98 x 98 cells. The resolution of the grid is set depending on the size of the area to be studied, typical grid resolution is 10 m in both x and y direction with a domain of interest covering an area of 1000 m by 1000 m. Bathymetry information from within the aquaculture lease was linearly interpolated into the structured grid system. DEPOMOD is forced with time series of ocean currents measured at one location. The current field is considered uniform over the whole grid. In the vertical, DEPOMOD accepts timeseries of up to five depth levels. All input information for the model is shown in Table 2.

The second module is the particle tracking module. This module uses particle information (water content, digestibility, percent wasted, carbon content, and settling velocity of feed particles; carbon content and settling velocity of feces) and cage information (size, depth, and amount of feed per cage) to compute the dispersion and location where deposition of particles onto the seafloor takes place. The different parameters defined in the particle tracking module are also presented in Table 2. Particle information is taken from literature (Chamberlain et al, 2005, Chamberlain and Stucchi 2007, Chang et al. 2014) and cage information from farm operator. Weekly feeding rates for each cage were obtained from the operator and converted into daily values before their use in the model.

Ocean current measurement was carried out some distance away from the aquaculture cages to ensure cage anchors did not perturb the ADCP signals. Since Site A is a bay presenting different orientations at different locations (Figure 1), the measured current velocity is first adjusted to the orientation of the channel at the location of the cage array. Hourly timeseries at five depth layers (the maximum number of current information accepted by DEPOMOD) were extracted from the data and used in the calculation of the deposition of waste falling from the cages. Considering the weekly feed information, the whole period of interest was also sectioned into weekly periods for which the timeseries of ocean currents were generated.

The third module is the resuspension module. This module computes the rate of deposition of particles at each model grid cell depending on whether resuspension of the particles due to strong near bottom current speeds is activated or not. In this version of DEPOMOD, resuspension is expected to occur when near bottom current speed is faster than ~9.5 cm s^{-1} (Cromey et al. 2002). In the present analysis, this module was also run with resuspension activated to evaluate the potential for dispersion of aquaculture waste farther beyond the cage array. In order to verify whether waste particles remain within the 1000 m x 1000 m grid (hereafter 1000-m domain), a test run was also carried out assuming a shallower uniform depth (few meters below the shallowest currents used to force the model) for the whole

domain and comparing the total amount of deposition with that from original bathymetry. The total amount of deposition at shallow depth provides information on the quantity of deposition one would expect should everything be deposited directly underneath the cage array; a larger amount of deposition than that computed using the real bathymetry translates into some particles being exported outside of the 1000-m domain of study. The model was subsequently run with a coarser grid (20 m x 20 m for a study area of 2000 m x 2000 m) to study dispersion and deposition of particles outside of the 1000-m domain.

In addition to the weekly run of the model, deposition flux was also computed for the same periods as the sediment trap data collection for comparison. The output of the deposition model was also compared with observations from the benthic survey (diversity, abundance, and presence or absence of bacterial mats).

3. RESULTS

3.1. ENVIRONMENTAL CONDITIONS

Figure 2 illustrates the profiles of temperature and salinity for winter (February) and fall (September) 2022. The whole water column was well mixed in February. In September, a mixed layer of ~25-30 m thick with temperature around 13°C, was observed below ~5 m depth with a ~50 m thick thermocline lying underneath. Temperature below 75 m depth was ~3°C in winter and slightly above 2°C during fall. Salinity in winter was ~32 within the whole water column except near the surface. In fall, a thin layer of brackish water, less than 5 m thick, was observed in the top surface. Beneath the brackish water, the salinity was above 31 and slightly increasing to ~32 towards the bottom.

3.2. CURRENT REGIME

Currents varied from the surface to the bottom. The main direction of the currents was along the orientation of the channel (Figure 3 for Site A and Appendix for Site B). At similar depth, current speeds were generally higher at Site B than at Site A. The maximum current speed measured at the nearest depth from the bottom was 24.5 cm s^{-1} and 18.5 cm s^{-1} at Site A and Site B, respectively. At the respective depth closest to the bottom, 2 % of the record at Site A (the value considered by DEPOMOD as the threshold above which resuspension will take place); and 1 % at Site B showed speed over 9.5 cm s^{-1}. The maximum duration the current speed was above this value was ~5 h at both sites. These currents are expected to generate resuspension of the particles deposited at the seafloor before they get resettled back. Table 3 summarizes the statistics of the ocean currents used to force DEPOMOD. Mid-depths tended to show lower median speeds as well as lower observed maximum current speeds than the near surface and the near bottom depths.

The total tidal contribution generally explains less than 12% of the variability of the currents with the near bottom currents having 5% or less tidal contribution. When looking at the temporal variability, the analysis of the data (Figure 4) shows monthly variability of the current speed at all depths for Site A. The variability at Site A for the upper 30 m layer (near surface) is illustrated in Figure 4 and that of the lower 30 m layer (near bottom) in Figure 5. Stronger median current speed was observed in the upper layer in March (4.6 cm s^{-1}), April (4.3 cm s^{-1}), and September (4.3 cm s^{-1}) while lower median speed (3.6 cm s^{-1}) was observed In July. July current speed also experienced the lowest variability compared with the other months (2.9 cm s^{-1}) as shown by the interquartile range, IQR (Figure 4). The observed maximum current speed was lowest in July and highest in April and September. For the current speed in the lower 30 m layer near the bottom (Figure 5), the median current speed was lower than that near the surface, the highest monthly median speed was also observed in March (3.4 cm s^{-1}) while the lowest in May

(3 cm s^{-1}). The current speed showed lower variability from the month of April to September (2.4 to 2.6 cm s^{-1}) and higher variability in March.

For Site B, the upper layer shows median speed between 4.9 and 5.9 cm s^{-1} with the higher values observed in winter and fall, similarly, current speed shows more variability in winter and fall. For the near seafloor layer, median speed was between 1.8 and 2.1 cm s^{-1} with higher speed and slightly higher variability in September (Appendix 1).

3.3. MEASURED DEPOSITION

Figure 6 and Figure 7 show photos of the sediment sample collected by each bottle at different dates for the stations near the cage edge. Each sample corresponds to the period specified in Table 1. Analysis of the chemical and biological content of the bottles is still ongoing but visually, one can see differences in the amount of materials collected at each time and at each site. For Site A, bottle #1 (period around 12 Mar. 2022), and bottle #8 (27 Sept. 2022) collected more materials. Bottles #2 and #7 collected some materials, and bottle #3 to #6 (beginning of May to beginning of Aug. 2022) collected a very small amount of materials. For Site B, large amount of material was collected with bottles #1, 2, 3, 7, and 8 while bottles #4 and 5 collected a very small amount of materials (Mid-May to end of June).

3.4. MODELED DEPOSITION

3.4.1. 1000 x 1000 m^2 domain

Typical simulation using DEPOMOD is carried out considering the deposition occurs within an area 500 m away from the center of the cage array, in this case the model configuration covers an area of 1000 m x 1000 m, centered at the middle of the cage array, with a resolution of 10 m x 10 m. With limited observed current speeds showing values above 9.5 cm s^{-1} (1-2% of near bed measurements, suggesting resuspension), the model was run without and with resuspension option. Figure 8 illustrates the modeled deposition at Site A and Site B for the week of 10-16 April 2022 when forced with ocean currents at five depth levels and without activating resuspension. The pattern of deposition followed the direction of the channel. The highest deposition area was generally found around the cage array, with a total amount decreasing away from the cage area. One can also observe patchy areas of very small deposition farther away. Total solid deposition of 1 to 10 g m^{-2} , after one week, has been found at a distance of 570 m from the cage array at site A and 510 m from the cage array at Site B. These amounts are rather small but confirm the possibility of deposition at a distance greater than 250 m away from the cages, a distance considered to be far-field. The amount of deposition under some cages was also small, less than 2 g m^{-2} after one week (cage in the southeast corner for Site A and the southernmost cages for Site B), principally because these cages did not hold any fish during the simulated week. Total amount of deposition under Site B was generally less than under Site A. The map also shows the possibility of some deposition happening outside the 1000-m domain for site B (Figure 8).

To quantify the proportion of deposition occurring outside of the 1000-m domain, we compared the amount of waste deposition with the expected total waste leaving the cages (Figure 9 and summarized in Table 4). The result shows that the percentage of waste leaving the 1000-m domain varied in time, with the variation not showing any specific seasonal pattern.

In spring, ~0.2 % (corresponding to 10 kg in weight for the specific week) or less of the total amount of modelled deposition at Site A was found outside of the 1000-m domain except at the end of May/early June 2022 when it was maximal and ~0.6 % (corresponding to ~33 kg) of the total. At Site B, the amount of waste leaving the domain was generally less than 1.5 % (less than 50 kg in weight) while at the end of May/early June 2022, ~6 % of the total waste (representing ~230 kg in weight) left the 1000-

m domain. With resuspension activated (Figure 20 in the Appendix), the percentage of waste leaving the domain, at site A, was generally less than 20 % (~700 kg or less in weight) while the maximum percentage of waste exported outside the 1000-m domain was ~60 % (corresponding to ~1600 kg in weight) and occurred mid-March. At the end of May/early June, ~25 % of the total deposition (~1400 kg) ended up outside of the simulated domain. For Site B, the amount of waste exported outside of the 1000-m domain was generally less than 4 % of the total deposition (< 75 kg in weight) while the highest exported amount was found to be ~48 % (~750 kg in weight) occurring in Mid-March. Note that the percentage and corresponding weight values are related to the amount of deposition for the specific week, not for the whole period of measurement.

3.4.2. 2000 x 2000 m^2 domain

To assess how far from the cage array the deposition can occur, the model was run with a coarser grid but larger area of study (20 m x 20 m grid making the study domain to 2000 m x 2000 m). Figure 10 illustrates the map of deposition from this coarser grid. As expected, the degree of details in the distribution of the deposition computed using the coarser grid is generally lower than that computed with the higher resolution model (Figure 9). The amount of deposition per square meter at each grid point under the cage array computed using this coarser grid is generally lower than that computed with the higher resolution model as the deposition tends to geographically spread within the surrounding area. The map shows deposition happening farther away (~1000 m away on both directions) from the cage for Site A and mainly towards the northwest part for Site B. Note that as with the 1000-m domain case-run, the ocean current data used to force this lower resolution model came from the same one-location measurement. Since DEPOMOD only allows current data from one location, the ocean current field used to do the calculation is horizontally uniform at each depth. Therefore, the spatial variation of the current field (in the horizontal) due to the bay configuration (winding channel) was not considered in the calculation. Thus, the result can only be used to qualitatively estimate the possibility of deposition outside of the 1000-m domain rather than to estimate the extent of deposition.

3.4.3. Varying the number of current levels (5-level vs. 3-level)

Simulation with three levels of ocean currents was also carried out to assess the effect of reducing the resolution of current information in the vertical on the area of deposition. The simulations were completed with 1000 m x 1000 m model domain. Figure 11 illustrates an example comparing the footprint at Site B where the total deposition corresponds to the Canadian Aquaculture Activity Regulation of 1-5 g C m^{-2} d^{-1} of deposited biochemical oxygen-demanding (BOD) matter. On week 15 (16 April 2022), the estimated footprint of the deposition of BOD matter is larger when computed using a timeseries of five levels of current (29 000 m^2) versus using three levels of current (15 000 m^2). A similar calculation was carried out every week from the beginning until the end of the period of measurement. The comparison of the footprint for each week shows that the runs forced with three levels of currents have smaller footprints than those forced with five levels of currents when the area of deposition was small while it resulted in larger footprints when the area of deposition was large (Figure 12). The maximum reduction in the area of deposition when using three levels of currents was ~27 % at Site A (week of 21 Aug 2022) and ~90 % at Site B (week of 20 March 2022), and the maximum increase in the area, when the deposition area is large, was 12 % at Site A (week of 19 Jun 2022) and ~9 % at Site B (week of 12 Jun 2022).

3.5. COMPARISON BETWEEN SEDIMENT TRAP MEASUREMENT AND MODEL OUTPUT

The total deposition was computed for the same periods of collection by each sediment trap bottle for comparison. Figure 13 compares the flux of deposition of material computed from the model with

1000-m domain with the collected organic matter using the sediment traps directly underneath the edge of the
cage array. Both sites show a decrease in collected deposition from late February to early May 2022. The rates of deposition of organic matter stayed low (under 1 g solid m^{-2} d^{-1}) until mid-September when it showed a slight increase.

As for the modeled deposition, the corresponding rates of deposition were low for Site B. By contrast, Site A started with rates of the same range as the observation (4 g solid m^{-2} d^{-1} for modelled rates and 3 g solid m^{-2} d^{-1} for observation on 12 March 2022) but on 22 March 2022, the model computed rates similar to the previous date; subsequent rates were higher in early May and early August (~6 g solid m^{-2} d^{-1} and above) and lower (~2 g solid m^{-2} d^{-1}) at the end of June. The modelled rates of deposition at Site A were always higher than the rates computed from the observation.

3.6. COMPARISON BETWEEN BENTHIC STRUCTURE AND SIMULATED DEPOSITION

A total of 112 and 121 stations were surveyed for site A and site B, respectively. The main taxa that were present are crabs, bottom shrimps, ball sponges, encrusting sponges and rearing forms, seastar, ophirids, crinoid, anemone, Metridium sp (anemone), soft coral, seapen and serpulids. Figure 14 and Figure 15 show the respective map of abundance and diversity observed during the benthic survey. No species were observed at 20 % and 12 % of the surveyed stations for Site A and Site B, respectively. About half of the surveyed stations in both sites showed one to five individuals per m^2 observed at each monitored location. Seven (Site A) and 14 (Site B) stations had 5 to 10 individuals per m^2. Also, only few locations showed higher abundance with 15-20/20-25 observed individuals per m^2 (6 stations at Site A and 10 stations at Site B).

In terms of diversity, the maximum number of taxa observed at each location was five (Site A) and seven (Site B). Most of the locations had 1-3 taxa present within a 50 x 50 cm^2 area (in total 58 % and 54 % of stations for Site A and Site B, respectively) with the lower diversity locations (only one or two different species) found at the deeper part of the domain. Bacterial mats were only observed at 6 % of the monitoring stations (7 out of 112 locations for Site A - four located at cage edge, and 7 out of 121 locations for Site B - all 7 located at the edge of the cage array).

When looking at the amount of deposition computed with DEPOMOD and its relation with observed abundance around each site (Figure 16), one can see that deposition around Site A ranged from 0 to ~1800 g solid m^{-2} while that around Site B ranged from 0 to ~800 g solid m^{-2}. No clear correspondence can be noted between the deposition and observed abundance. Fauna were observed at locations with deposition ranging from 0 to ~800 g solid m^{-2} in the vicinity of both sites. However, some locations with deposition ranging from 0 to 1800 g solid m^{-2} at Site A and ranging from 0 to 75 g solid m^{-2} at Site B did not show any observed species.

4. DISCUSSION

4.1. ENVIRONMENT CONDITIONS

The profile of salinity in the domain shows the presence of freshwater near the surface. The low salinity water comes from freshwater run-off likely present from Spring to Fall, and is found only in the upper 5 m near the surface; such run-off is not present or is very minimal in Winter. In the fall, there is a ~35 m thick warm mixed layer and a thick thermocline (above ~75 m depth) combined with a low salinity in the very thin layer near the surface. This suggests that the water in the upper 75 m is warmed by exchange of heat from the surface, exchange of heat and warmer water from the shelf region and/or their

combination. Farmer and Freeland (1983) reported that water exchange between continental shelf and fjords can happen at any depth from surface to bottom due to wind, tides, water density differences, and internal processes. These processes together with the complex configuration of the fjord is expected to affect the ocean current structure both horizontally and vertically and thus the deposition of farming wastes. The effect changes depending on the season resulting in the ocean currents being more dynamic in Fall (Donnet et al 2022). In their study of another bay in the same region, Donnet et al (2022) also reported signs of layering processes throughout the year with more current pulse events in the upper layer associated with the presence of stratification observed in summer. Our measurement showed stronger currents in winter and in fall and weaker currents in summer at both sites with different variability of the current speed in the vertical depending on the season (Figures 4, 5, 18, 19) underlying the regional character of the oceanographic conditions.

4.2. MODELLING WITH A 1000 x 1000 m^2 DOMAIN

Modeling the dispersion, sinking, and deposition of particles released from an open-net farm activity presents various challenges, as it relies on information such as sinking velocity of particles released from the cages and ocean currents that are used to transport the particles around and away from the cages (Symonds 2011 and Bannister et al 2016) among others. Using the parameters defined in Table 2 and the current measurements at the two sites, our calculation demonstrated higher deposition in the area close to the cage array. This high deposition has been associated with fast sinking particles which are mostly made up of feed waste (Chamberlain and Stucchi 2007), feed waste having higher density (in comparison to feces) and having not absorbed water to sufficiently affect its density (Piedecausa et al, 2009) before reaching the seafloor. The amount of modelled deposition decreased with increasing distance from the cage array and our results also showed that particles were exported outside of the 1000-m study domain, over some weeks, without any specific seasonal pattern, or whether resuspension was activated or not in the model configuration. The maximum amount of deposition exported much farther from the cage array was 0.6 to 6 % of the total deposition when the model was run without resuspension. While studies such as Ali et al (2011) concluded the necessity to consider the model with resuspension to study far-field deposition, our model run showed that as much as 48-60 % of the falling particles could be exported outside of the 1000-m domain under the same consideration; these maximum exports happened mid-March when a storm event with strong currents was observed all over the water column. Previous Canadian studies carried out in British Columbia and in New-Brunswick found that DEPOMOD tends to overestimate the amount of particle transport caused by resuspension (Chamberlain and Stucchi 2007, Chang et al. 2012). This led Chamberlain and Stucchi (2007) to consider simulations with resuspension unrealistic and Chang et al. (2012) to state that the threshold current speed for resuspension (the 9.5 cm s^{-1} speed) might be inappropriate for the southwest coast of New- Brunswick. This might also be the case for the present model analysis of deposition around deep-water farms.

In terms of comparing both sites, the modelled rate of deposition (Figure 13) at Site B was lower than that at Site A. Food inputs at Site A were higher than at Site B (Figure not shown) and would have resulted in higher waste amount leaving the net pens. Ocean currents at Site B were also faster in the upper 100 m, leading to the falling particles being transported farther away from the release sources during their sinking process and thus reducing the amount of deposition (and the corresponding rates) computed directly underneath the cages at that site. These two factors and their combination would explain the differences in the computed rate of deposition between the two sites.

4.3. MODELING WITH A 2000 x 2000 m^2 DOMAIN

To understand the deposition occurring outside of the 1000-m domain, simulation with a larger area (2000 m x 2000 m) was required. DEPOMOD including a larger domain has a coarser grid system but uses a one-point current data for the whole large domain and, by default, assumes uniform currents everywhere within the domain of study. From this run, deposition occurring farther than 500 m away from the site had a tendency to happen along one main direction with minimal effect due to the shape of the channel. As ocean current field is known to be complex in fjord systems (Asplin et al. 2011, 2014) and that the study area bay presents a winding channel with changes of orientation within the area surrounding the cage array, it is expected that the ocean current field would be affected by these features. Spatially variable currents will transport particles along the winding channel before they settle to the bottom. Without a spatially varying current field used as forcing, although the model may be used to compute the amount of particles released from the farm, the spatial distribution of the particles deposition is not subject to the changes in the orientation of the channel and in the ocean currents along the channel and may not happen at the right location. Assuming that ocean currents are uniform everywhere in the domain by using a one-point current data to represent the whole field can be too crude of an approximation (Asplin et al. 2011, 2014, Broch et al 2017). To better model particle dispersion and deposition, one needs to have access to spatially variable ocean current field and the model needs to accept these non-uniform currents (Page et al 2023).

4.4. MODEL *vs.* MEASURED DEPOSITION

With respect to the comparison of the estimated model deposition with measured deposition from sediment traps, discrepancy is observed with estimated deposition at Site A higher than the measurements while it is lower at Site B (model deposition was ~1.3 times higher at the beginning to ~80 times higher by August 2022 for Site A and ~60 times lower at the beginning to ~15 times lower by May 2022 for Site B). The total deposition near the cages computed by the model is related to the amount of feed given to the fish which can change in time depending on the farm operator's husbandry practices. In contrast, the organic matter collected by the sediment traps, as per our measurement, shows patterns not related to feeding practices, this would be explained by the presence of relatively strong currents at some depth(s) which transported the particles away from the traps while sinking. As the model can only use current information at maximum five depth levels, these strong currents might not have been well represented in the model configuration. This discrepancy between the observation and the model output suggests limitations in how the model simulates the dispersion and deposition processes. Part of the discrepancy which is due to the model not considering the current variability is explained further below.

The model assumes that the deposition process is driven by physics related to the presence of ocean currents, ocean turbulence, and gravitation. Model simulations with three and five levels of currents show differences in the geographic distribution of the deposition. Similar to other locations in the region (Ratsimandresey et al. 2019), the ocean currents in this fjord present complex layering; thus the use of few vertical levels of currents, to drive particle dispersion, does not consider the whole variability of the ocean currents in the vertical which results in the sinking particles not subject to displacement caused by the varying horizontal velocities present at different depths. Cromey et al. (2002) stated that good deposition modelling would be achieved by using multiple layers of accurate current information. This leads to changes in the horizontal transport at different layers before the particles reach the seafloor (Nooteboom et al. 2020), and may result in a deviation from the observation of the location of deposition.

Sinking rates of the waste particles are determined by many factors including particles property as well as that of the water in which they settle: feed pellets get less dense the longer they are immersed resulting in decreasing sinking rates (Piedecausa et al, 2009), larger feed pellets were reported to sink faster than smaller one (Skøien, 2017, Skøien et al. 2016, Vassallo et al. 2006); the sinking rates for fecal pellets also vary depending on the size class of the farmed fish with larger fish generally having larger and lighter fecal pellets (Bannister et al 2016) resulting in slower sinking rates. The distribution of particle sinking rates with respect to the type and size of particles released from aquaculture farm operation was not quantified in our study. Page et al. (2023) did a review of the sinking rates that previous studies have used for feed particles and for feces. They reported substantial variation with values ranging between 2 to 17 cm s^{-1} for feed particles and 0.7 to 10 cm s^{-1} for fecal particles, the rates can also vary depending on the size and mass of the particles in the same study. The selection of the distribution of the sinking rates has an important effect on the period of sinking. Table 5 shows an order of magnitude difference in the time necessary for particles to reach the bottom for different depths and different sinking rates: fecal particles experiencing a sinking rate of 0.7 cm s^{-1} take ~6 h to reach a 150 m depth seafloor and ~11 h to reach a 270 m depth seafloor while for a fast sinking rate of 10 cm s^{-1}, the time necessary to reach the seafloor is approximately 24 and 45 minutes for a 150 and a 270 m depth water, respectively. In a region where the currents can rapidly change (in time and in the vertical), this consequently affects how far particles are horizontally transported during the sinking process and thus results in variation in the location of deposition. This will be the case for high and low energy sites (Currie 2022).

Chang et al (2014) stated that when using resuspension process in the simulation of deposition with DEPOMOD, the prediction tends to underestimate areas of elevated deposition rates. Keeley et al (2013) also concluded that DEPOMOD might oversimplify the association between current flow, sediment resuspension and ecological impact. Comparison with the result from Keeley et al. (2013) and Chang et al. (2014) might not be straightforward, because their study was for sites with 27 to 40 m and for 26 m depth, respectively, while the present model run was carried out at sites 150 and 270 m depth. Nonetheless, it is expected that the association between current flow, sediment resuspension and ecological impact is even more complex in such deep sites with complex current structure. With those depths, and with a settling velocity of 8.3 cm s^{-1} for feed particles and 3.2 cm s^{-1} for feces, a free falling particle will take 30 minutes (for feed) and 78 minutes (for feces) to reach the seafloor at Site A (54 minutes for feed and 140 minutes for feces at Site B). Thus, feed waste and excretion (as defined in DEPOMOD) would be at the seafloor at most two hours and a half after release. During this period, DEPOMOD uses simplified parameters/inputs: it assumes that the ocean currents were horizontally uniform, that the variability of the currents in the vertical was represented by at most only five levels of current timeseries, and that the waste particles sank with similar settling velocity distribution over the whole water column. Given the differences between the DEPOMOD-computed deposition flux and that measured by the sediment traps , we conclude that DEPOMOD lacks of the sufficient details to model the deposition around sites in deep areas.

Given the limitation that DEPOMOD has in simulating dispersion and deposition of particles around sites with a spatially complex ocean current field, other more complex models (or coupled models), with higher grid resolution, might be more suitable in particular for winding fjords (Ali et al 2013). Broch et al. (2017), for example, used a coupled dispersion model DREAM/3D-hydrodynamic model SINMOD to predict waste deposition from aquaculture activity. An improvement of DEPOMOD, called NewDEPOMOD, has also been developed (SRSL 2021); this newly redesigned model can be forced with currents from 3D hydrodynamic model (e.g. FVCOM as in Rochford et al 2017) or with current

observations at various locations. Some main features of NewDEPOMOD include the possibility to compute far-field deposition using 3D variable current information in a variable seabed topography and at high resolution. NewDEPOMOD, however, still needs considerable site-specific tuning in order to model particle resuspension and transport (Fox et al. 2023)

4.5. VIDEO SURVEY

Richness and abundance of species around aquaculture farms are expected to be affected by the fluxes of matter from the aquaculture activity (e.g. Kutti et al 2007, Keeley et al 2013, Hamoutene et al 2016, Dunlop et al 2021). Dunlop et al (2021), in a study of three deep sites in Norway, showed that the benthic epifaunal community composition is affected by the total particulate matter (TPM) flux. The TPM fluxes were high near the cage and decreased farther away. They observed an increasing abundance of lugworms and seastar as they get closer to the farms, while the density of sponges and soft coral near the cages was relatively low. From our survey, no easily identifiable pattern was observed for the geographic distribution of abundance and diversity. The survey did not show clear differences in abundance and diversity of species between areas near the aquaculture cages and those farther away. It is not clear whether this is due to the site being very deep, to the small area sampled (i.e. number of videos and area covered by video surveys), to the patchiness of deposition and of the benthos type, or combinations of all these conditions. While the composition and density of the sponges observed at the Norwegian sites (Dunlop et al 2021) were considered rich and high, our survey showed low species diversity and abundances with patchy distribution in the whole area similar to other aquaculture regions in Newfoundland (Hamoutene et al 2015, 2016, 2018; Salvo et al 2017, 2018). The patchy distribution might be an important factor in explaining the difficulty to find a clear relationship between species abundance/richness and survey location; larger images (from the underwater camera) per station may be required in order to disclose a better identification of species that will help overcome the difficulty to interpret data in NL environments with such low density. The benthic sampling as designed can only allow the detection of effects associated with end of production (anoxic conditions, presence of indicators) and its limitation in identifying more subtle benthic changes has been documented (Salvo et al. 2017; Hamoutene et al. 2018). In our study, leases were not fully stocked (not all the planned cage area was used) and surveys were undertaken after one year and few months of production, therefore visualization of effects may have been hindered by the fact that effects were more subtle and not captured by the videos, or that the surveys did not occur in the locations where the deposition may have occurred. Also any relation between species abundance and deposition cannot be concluded either, given the potential shortcoming for DEPOMOD to geographically model the deposition.

Despite the above, the presence of bacterial mats directly underneath the edge of the cage indicates an effect of the organic enrichment associated with the aquaculture activity (Hamoutene et al 2016). Hamoutene et al (2016) have found such mats to occur mainly within 10 m from the cages and their presence has been shown to reflect a shift in bacterial community composition as a result of organic enrichment (Dowle et al. 2015, Salvo et al 2017). Salvo et al (2017) have found that the changes can happen within one month of production.

From a regulatory point of view, the Canadian framework (the Canadian Aquaculture Activities Regulations, AAR 2015) establishes that sites showing the presence of bacterial mats, aggregates of opportunistic polychaete (OPC), and/or barren substrates in more than 70 % of the locations specified in the monitoring standard are not to be restocked. Site A and Site B only had less than ~26 % of the monitored stations showing bacterial mats or barren substrate thus they are fully compliant from the AAR perspective.

5. CONCLUSION

The analysis shows that DEPOMOD presents limitation in modelling accurately the dispersion and geographic distribution of near-field deposition of waste particles around deep sites located in areas with ocean currents having complex spatial variability. This is in part due to DEPOMOD accepting limited information with respect to ocean currents used to force the model (this includes using current measurements at only one location for the whole domain of analysis and allowing only a few vertical current data measurements which does not consider the full vertical structure of the water column). Consequently, it cannot reproduce distribution of far-field deposition either. Such limitations result in the difficulty in anticipating the potential relationship between waste deposition around aquaculture sites and benthic impacts. The use of more complex hydrodynamic-deposition model with realistic ocean current forcing is recommended to study the geographic distribution of aquaculture waste in the Newfoundland deep site context.

ACKNOWLEDGEMENTS

A number of individuals and groups were involved in supporting this study. We would like to thank all the scientist and technical crew who helped collect all the data used in the analysis, in particular Ed Horne, Shannon Cross, Matthew Grandy, and MOWI crew. This study was supported by the Aquaculture Collaborative Research and Development Program (ACRDP). Finally, we would like to thank Adam Drozdowski and Pramod Thupaki for their thorough and thoughtful reviews that greatly improved this report.

REFERENCES

AAR (2015). Aquaculture Activities Regulations guidance document website. http://www.dfo-mpo.gc.ca/aquaculture/management-gestion/aar-raa-gd-eng.htm. (Accessed Jan 2025).

Ali, A., Thiem, Ø., & Berntsen, J. (2013). Numerical simulation of flow and aquaculture organic waste dispersion in a curved channel. Ocean Dyn. 63, 1073–1082.

Ali, A., Thiem, Ø., & Berntsen, J. (2011). Numerical modelling of organic waste dispersion from fjord located fish farms. Ocean Dyn 61:977–989.

Asplin, L., Boxaspen, K., & Sandvik, A. D. (2011). Modeling the distribution and abundance of planktonic larval stages of lepeophtheirus almonis in Norway. In Salmon lice an integrated approach to understanding parasite abundance and distribution, pp. 31–50. Ed. By S. Jones, and R. Beamish. John Wiley & Sons.

Asplin, L., Johnsen, I. A., Sandvik, A. D., Albretsen, J., Sundfjord, V., Aure, J., & Boxaspen, K. K. (2014). Dispersion of salmon lice in the hardangerfjord. Marine Biology Research, 10: 216–225.

Bannister, R.J., Johnsen I.A., Hansen, P.K., Kutti, T., & Asplin, A. (2016). Near- and far-field dispersal modelling of organic waste from Atlantic salmon aquaculture in fjord systems, ICES Journal of Marine Science, Volume 73, Issue 9, Pages 2408–2419, https://doi.org/10.1093/icesjms/fsw027.

Broch, O.J., Daae, R.L., Ellingsen, I.H., Nepstad, R., Bendiksen, E.Å., Reed, J.L., & Senneset, G. (2017). Spatiotemporal dispersal and deposition of fish farm wastes: a model study from central Norway. Front Mar Sci 4: 199.

Chamberlain, J. & Stucchi, D. (2007). Simulating the effects of parameter uncertainty on waste model

predictions of marine finfish aquaculture. Aquaculture 272: 296−311.

Chamberlain, J., Stucchi, D., Lu, L., & Levings, C. (2005). The suitability of DEPOMOD for use in the management of finfish aquaculture sites, with particular reference to Pacific Region. DFO (Fisheries and Oceans Canada) Canadian Science Advisory Secretariat Res Doc 2005/035, Dartmouth. Available at https://www.dfo-mpo.gc.ca/CSAS/Csas/DocREC/2005/RES2005_035_e.pdf (accessed March 2014).

Chang, B.D., Page, F.H., Losier, R.J., & McCurdy, E.P. (2014). Organic enrichment at salmon farms in the Bay of Fundy, Canada: DEPOMOD predictions versus observed sediment sulfide concentrations. Aquacult. Environ. Interact. 5, 185–208.

Chang, B.D., Page, F.H., Losier, R.J., & McCurdy, E.P. (2012). Predicting organic enrichment under marine finfish farms in southwestern New Brunswick, Bay of Fundy: Comparisons of model predictions with results from spatially-intensive sediment sulfide sampling. DFO Can. Sci. Advis. Sec. Res. Doc. 2012/078. Iv + 146 p.

Cromey, C., Nickell, T., & Black, K. (2002). DEPOMOD - modelling the deposition and the biological effects of wastes solids from marine cage farms. Aquaculture 214,211 - 239.

Cromey, C.J. & Black, K.D. (2005). Modelling the impacts of finfish aquaculture. In: Hargrave BT (ed) Environmental effects of marine finfish aquaculture. Handbook of environmental chemistry, Vol 5, Part M. Springer-Verlag, Berlin, p 129−156.

Currie, M. (2022). Investigating uncertainty and emulating process based models with multivariate outputs, applied to aquaculture. PhD thesis. pp 210.

DFO (2009). Water currents, drifter trajectories and the potential for organic particles released from Little Musquash Cove to enter the Musquash MPA. DFO Can. Sci. Advis. Sec. Sci. Resp. 2009/001. Retrieved January 2018.

DFO (2012). Standard operating procedures (SOP) for underwater video camera system. https://waves-vagues.dfo-mpo.gc.ca/library-bibliotheque/347683.pdf (Accessed May 2024).

DFO (2014). Potential impacts of finfish aquaculture on hard bottom substrates and development of a standardized monitoring protocol. DFO Can. Sci. Advis. Sec. Sci. Advis. Rep. 2014/017.

DFO (2022). DFO Newfoundland and Labrador Region Science Review of Three Proposed Marine Harvest Atlantic Canada Marine Finfish Aquaculture Facilities in Chaleur Bay, Newfoundland. DFO Can. Sci. Advis. Sec. Sci. Resp. 2022/044.

Doglioli, A.M., Magaldi, M.G., Vezzulli, L., & Tucci, S. (2004). Development of a numerical model to study the dispersion of wastes coming from a marine fish farm in the Ligurian Sea (Western Mediterranean). Aquaculture 231, 215-235.

Donnet, S., Cross, S., Goulet, P., and A.W Ratsimandresy. (2018a). Coast of Bays Seawater Vertical and Horizontal Structure (2009-13): Hydrographic Structure, Spatial Variability and Seasonality Based on the Program for Aquaculture Regulatory Research (PARR) 2009-13 Oceanographic Surveys. DFO Can. Sci. Advis. Sec. Res. Doc. 2017/077. viii + 255 p.

Donnet, S., Ratsimandresy, A.W., Goulet, P., Doody, C., Burke, S. & S. Cross. (2018b). Coast of Bays Metrics: Geography, Hydrology and Physical Oceanography of an Aquaculture Area of the South Coast of Newfoundland. DFO Can. Sci. Advis. Sec. Res. Doc. 2017/076. x + 109 p.

Donnet, S., Lazure, P., Ratsimandresy, A., & Han, G. (2020). A comprehensive oceanographic dataset of a subpolar, mid-latitude broad fjord: Fortune Bay, Newfoundland, Canada. Earth Syst. Sci. Data 12, 1877–1896. http://dx.doi. org/10.5194/essd-12-1877-2020.

Donnet, S., Lazure, P., Ratsimandresy, A., & Han, G. (2022). The physical oceanography of Fortune Bay, an overview. Regional Studies in Marine Science, 56, 102698. https://doi.org/10.1016/j.rsma.2022.102698, https://archimer.ifremer.fr/doc/00800/91241/.

Dowle, E., Pochon, X., Keeley, N., & Wood, S.A. (2015). Assessing the effects of salmon farming seabed enrichment using bacterial community diversity and high-throughput sequencing. FEMS Microbiol Ecol 91:fiv089.

Dunlop, K., Harendza, A., Bannister, R., & Keeley, N. (2021). Spatial response of hard- and mixed-bottom benthic epifauna to organic enrichment from salmon aquaculture in northern Norway. Aquaculture Environment Interactions, 13, 455.

Farmer, D.M. & Freeland, H.J. (1983). The physical oceanography of fjords. Prog. Oceanogr. 12, 147–219. http://dx.doi.org/10.1016/0079-6611(83)90004-6.

FAO. (2018). The State of World Fisheries and Aquaculture 2018 – Meeting the sustainable development goals. Rome.

Fox, C., Webb, C., Grant, J., Brain, S., Fraser, S., Abell, R., & Hicks, N. (2023). Measuring and modelling the dispersal of salmon farm organic waste over sandy sediments. Aquaculture Environment Interactions, 15, 251-269.

Gowen R.J. & Bradbury N.B. (1987). The ecological impact of salmonid farming in coastal waters: a review. Oceanography and Marine Biology Annual Review 25:563–575.

Hamoutene, D., Salvo, F., Belley, R., Lush, L., Hendry, C., & Marshall, K. (2017). An evaluation of benthic monitoring baseline assessments completed as part of the regulatory requirements for aquaculture finfish site applications on the South Coast of Newfoundland. Can. Tech. Rep. Fish. Aquat. Sci. Fs97-6/3222E-PDF: v + 25 p.

Hamoutene, D., Salvo, F., Bungay, T., Mabrouk, G., Couturier, C., Ratsimandresy, A., & Dufour, S.C. (2015). Assessment of Finfish Aquaculture Effect on Newfoundland Epibenthic Communities through Video Monitoring. North American Journal of Aquaculture, 77:2, 117-127, DOI: 10.1080/15222055.2014.976681.

Hamoutene, D., Salvo, F., Cross, S., Dufour, S.C., & Donnet, S. (2018). Linking the presence of visual indicators of aquaculture deposition to changes in epibenthic richness at finfish sites installed over hard bottom substrates. Environmental Monitoring and Assessment, 190.

Hamoutene. D., Salvo, F., Donnet, S., & Dufour, S.C. (2016). The usage of visual indicators in regulatory monitoring at hard-bottom finfish aquaculture sites in Newfoundland (Canada). Mar Pollut Bull 108:232−241.

Hargrave, B.T., Filgueira, R., Grant, J., & Law, B.A. (2022). Combined models of growth, waste production, dispersal and deposition from cage-cultured Atlantic salmon to predict benthic enrichment. Aquacult Environ Interact 14:309-328. https://doi.org/10.3354/aei00445

Henderson, A.R. & Ross, D.J. (1995). Use of macrobenthic infaunal communities in the monitoring and

control of the impact of marine cage fish farming. Aquacult. Res. 26, 659–678.Kalantzi I, Karakassis I. (2006) Benthic impacts of fish farming: Metaanalysis of community and geochemical data. Mar Pollut Bull. 52(5):484-493.

Keeley, N.B., Cromey, C.J., Goodwin, E.L., Gibbs, M.T., & Macleod, C.M (2013). Predictive depositional modelling (DEPOMOD) of the interactive effect of current flow and resuspension on ecological impacts beneath salmon farms. Aquacult. Environ. Interact., 3, 275-291.

Keeley, N.B., Forrest B.M., Crawford C., & MacLeod C.K. (2012). Exploiting salmon farm benthic enrichment gradients to evaluate the regional performance of biotic indices and environmental indicators. Ecological Indicators, 23.

Keeley, N.B., Valdemarsen, T. B., Woodcock, S., Holmer, M., Husa, V., & Bannister, R. J. (2019). Resilience of dynamic coastal benthic ecosystems in response to large-scale finfish farming. Aquaculture Environment Interactions, 11, 161-179. https://doi.org/10.3354/aei00301.

Kutti, T., Hansen, K.P., Ervik, A., & Høisæter, T. & Johannessen, P. (2007). Effects of organic effluents from a salmon farm on a fjord system. II. Temporal and spatial patterns in infauna community composition. Aquaculture 262:355−366.

Law B.A. & Hill P.S. (2019). Spatial and temporal variation in cumulative mass eroded and organic matter percentage in surface sediments near areas of active salmon aqua- culture. Aquacult Environ Interact 11:305−320.

Law, B. A., Hill, P. S., Maier, I., Milligan, T. G., & Page, F. (2014). Size, settling velocity and density of small suspended particles at an active salmon aquaculture site. Aquacult. Environ. Interact. 6, 29–42. doi: 10.3354/aei00116.

Mabrouk, G., Bungay, T., Drover, D., & Hamoutene, D. (2014). Use of remote video survey methodology in monitoring benthic impacts from finfish aquaculture on the south coast of Newfoundland (Canada). DFO Canadian Science Advisory Secretariat Research Document 039 v + 15p.

Nelson W.G. (2020). A quantitative assessment of organic carbon content as a regional sediment-condition indicator. Ecol Indic. 2019;114:106318.

Nooteboom, P.D., Delandmeter, P., van Sebille, E., Bijl, P.K., Dijkstra, H.A., & von der Heydt, A.S. (2020). Resolution dependency of sinking Lagrangian particles in ocean general circulation models. PLoS ONE 15(9): e0238650. https://doi.org/10.1371/journal.pone.0238650.

Page, F.H., Chang, B., Losier, R., & McCurdy, P. (2009). Water Currents, Drifter Trajectories, and the Estimated Potential for Organic Particles Released from a Proposed Salmon Farm Operation in Little Musquash Cove, Southern New Brunswick to Enter the Musquash Marine Protected Area. DFO Can. Sci. Advis. Sec. Res. Doc. 2009/003. Vi + 41 p.

Page, F.H., O'Flaherty-Sproul, M.P.A., Haigh, S.P., Chang, B.D., Wong, D.K.H., & Beattie, M.J. (2023). Modelling and Predicting Ecosystem Exposure to In-Feed Drugs Discharged from Marine Fish Farm Operations: An Initial Perspective. DFO Can. Sci. Advis. Sec. Res. Doc. 2023/001. Iv + 49 p.

Piedecausa, M. A., Aguado-Giménez, F., García-García, B., Ballester, G., & Telfer, T. (2009). Settling velocity and total ammonia nitrogen leaching from commercial feed and faecal pellets of gilthead seabream (Sparus aurata L. 1758) and seabass (Dicentrarchus labrax L. 1758). Aquaculture Research, 40,

1703-1714.

Podemski, C.L., Wlasichuk, C.A., Smith, E.L., Raper, J.L., & Azevedo, P.A. (2022). Validation of the Depositional Model DEPOMOD in the Freshwater Environment. Can. Tech. Rep. Fish. Aquat. Sci. 3468: xxxvii + 384 p.

Ratsimandresy, A.W., Donnet, S., & Goulet,P. (2019). Identification of geographic zones of influence associated with surface circulation for Aquaculture Bay management area application, Journal of Marine Systems, 204, 103291. https://doi.org/10.1016/ j.jmarsys.2019.103291

Rector, M.E., Weitzman, J., Filgueira, R., & Grant, J. (2021). Environmental indicators in salmon aquaculture research: A systematic review. Rev Aquacult. 14: 156–177. https://doi.org/10.1111/raq.12590.

Rochford, M. Aleynik, D., Gillibrand, P., & Black, K. (2017). The implementation of an FVCOM driven hydrodynamic model coupled with NewDEPOMOD in Scottish Aquaculture. Paper presented at Aquaculture Europe, Dubrovnik, Croatia, 17–20 October 2017.

Salvo, F., Mersereau, J., Hamoutene, D., Belley, R., & Dufour, S.C. (2017). Spatial and temporal changes in epibenthic communities at deep, hard bottom aquaculture sites in Newfoundland. Ecol Indic. 76:207-218.

Salvo, F., Oldford, V., Bungay, T., Boone, C., & Hamoutene, D. (2018). Guide for video monitoring of hard bottom benthic communities of the south coast of Newfoundland for aquaculture impact assessments. Can. Tech. Rep. Fish. Aquat. Sci. Fs 97-13/1284E-PDF: ix + 41 p.

SAMS. (2005). Ecological effects of sea lice medicines in Scottish sea lochs. Aberdeen, UK: SAMS (Scottish Association for Marine Science), Plymouth Marine Laboratory, Fisheries Research Services.

SEPA. (2005). Regulation and monitoring for marine cage fish farming in Scotland. Annex H: Methods for modelling in-feed anti-parasitics and benthic effects. Edinburgh, UK: SEPA (Scottish Environmental Protection Agency). Accessed April 2024.

Silvert, W. & Sowles, J. (1996). Modelling environmental impacts of marine finfish aquaculture. Journal of Applied Ichthyology 12, 75–81.

Skøien, K.R. (2017). Feed Distribution in Large Scale Sea Cage Aquaculture: Experiments, modelling and simulation. Doctoral theses at NTNU;2017:14. pp 201.

Skøien, K. R., Aas, T. S., Alver, M. O., Romarheim, O. H., & Alfredsen, J. A. (2016). Intrinsic settling rate and spatial diffusion properties of extruded fish feed pellets. Aquacultural Engineering, 74:30–37, ISSN 0144-8609. doi: http://dx.doi.org/10.1016/j.aquaeng.2016.05.001.

SRSL (SAMS Research Services Limited) (2021). NewDEPOMOD user guide. Scottish Association for Marine Science, Oban.

Stucchi, D., Sutherland, T.A., Levings, C., & Higgs, D. (2005). Near-field depositional model for salmon aquaculture waste. In: Hargrave BT (ed) Environmental effects of marine finfish aquaculture. Handbook of environmental chemistry, Vol 5, Part M. Springer-Verlag, Berlin, p 157−180.

Symonds, A.M. (2011). A comparison between far-field and near-field dispersion modelling of fish farm particulate wastes. Aquacult. Res., 42, 73-85.

Urbina, M.A. (2016). Temporal variation on environmental variables and pollution indicators in marine sediments under sea Salmon farming cages in protected and exposed zones in the Chilean inland Southern Sea. Science of the Total Environment, 573.

Vassallo, P., Doglioli, A.M., Rinaldi, F., & Beiso, I. (2006). Determination of physical behaviour of feed pellets in Mediterranean water. Aquacult Res 37: 119−126.

Weise, A.M., Cromey, C.J., Callier, M.D., Archambault, P., Chamberlain, J., & McKindsey, C.W. (2009). Shellfish-DEPOMOD: Modelling the biodeposition from suspended shellfish aquaculture and assessing benthic effects. Aquaculture 288(3–4): 239–253.

Wentworth, C.K. (1922). A scale of grade and class terms for clastic sediments. The journal of geology 30(5), 377–392.

TABLES

Table 1: Schedule for the programmable sediment traps for both Site A and Site B.

Bottle #	Days of Collection	Date (Mid Pt Collection)
1	10	2022-03-12 12:00
2	10	2022-03-22 12:00
3	10	2022-05-03 12:00
4	10	2022-05-13 12:00
5	10	2022-06-24 12:00
6	10	2022-08-05 12:00
7	10	2022-09-16 12:00
8	10	2022-09-27 12:00

Table 2: Parameter values used in the DEPOMOD model.

Grid generation module	
Grid cell dimensions (major and minor grids)	10 m x 10 m
Number of major grid cells	99 x 99
Number of minor grid cells	98 x 98
Material type	Total deposition
Release type	Continuous release of feed
Particle tracking module	
Particle information	
Food water content	10 %
Food digestibility 90%	90 %
Food wasted as % of food fed (default value) 3%	3 %
Carbon as % of feed pellets (dry weight)	57%
Carbon as % of feces (dry weight)	33 %
Settling velocity of feed pellets	Mean 8.3 cm s, STD 1.5 cm s^{-1}
Settling velocity of feces	Mean 3.2 cm s, STD 1.1 cm s^{-1}
Current velocity data	
Current velocity layers	3-5 layers within the water column, regularly distributed
Turbulence model	
Random walk model	Yes
Dispersion coefficient x 0.100 m^2 s^{-1}	0.100 m^2 s^{-1}
Dispersion coefficient y 0.100 m^2 s^{-1}	0.100 m^2 s^{-1}
Dispersion coefficient z 0.001 m^2 s^{-1}	0.001 m^2 s^{-1}
Particle trajectory model (default)	
Number of particles (for each particle type, per cage, at every model time step)	10
Trajectory evaluation accuracy (model time step)	High (60 s)
Current velocity time step	3600 s
Resuspension module	
Number of loops for which to run the model (Cromey et al. 2000)	2
Consolidation time of particles (default value)	4 d
Critical erosion threshold (non-adjustable)	9.5 cm s^{-1}

Table 3: Basic statistics of the currents at various depths for Site A and Site B for the period of 27 February 2022 to 27 September 2022. (*) Current directions have been adjusted to the direction of the channel where the cage arrays are located. Note that currents did not show any specific main direction for Site B at 147 and 205 m depths.

Site A					Site B				
Depth [m]	**Median speed [cm/s]**	**Main dir.***	**Max speed [cm/s]**	**Dir.* max speed**	**Depth [m]**	**Median speed [cm/s]**	**Main dir.***	**Max speed [cm/s]**	**Dir.* max speed**
25	3.5	NNW,SE	25.1	E	31	4.9	NNW, SSE	35.2	NNW
55	3.	NNW, SSW	13.	NW	89	3.	NNW, SSE	21.3	NWW
84	3.	NNW, SWW	13.8	NNW	147	2.8		14.9	N
114	3.1	W,NWW	16.9	SWW	205	3.		19.5	N
134	3.4	NW to SW	24.3	NNW	264	2.	NNE, SW to SE	20.0	SWW

Table 4: Main findings summarizing the amount of deposition (in percentage and in weight) exported outside of the 1000-m domain for runs with and without resuspension.

No resuspension						
	Most weeks			**Specific period/Outlier**		
Site	**Percentage outside of the 1000-m domain per week**	**Corresponding weight**		**Period**	**Percentage outside of the 1000-m domain per week**	**Corresponding weight**
A	< 0.2 %	< 10 kg		End May/Early June	0.6 %	33 kg
B	< 1.5 %	< 50 kg		End May/Early June	6 %	230 kg
With resuspension						
A	< 20 %	< 700 kg		End May/Early June	25 %	1400 kg
				Mid-March	60 %	1600 kg
B	< 4 %	< 75 kg		End May	6 %	230 kg
				Mid-March	48 %	750 kg

Table 5: Time [hour] necessary for a particle to fall from the surface and reach the bottom as a function of depth and sinking rates.

	Sinking rate [cm s^{-1}]	0.7	2	10	17
Depth [m]					
150		5.9 h	2. h	0.4 h	0.25 h
270		10.7 h	3.75 h	0.75 h	0.4 h

FIGURES

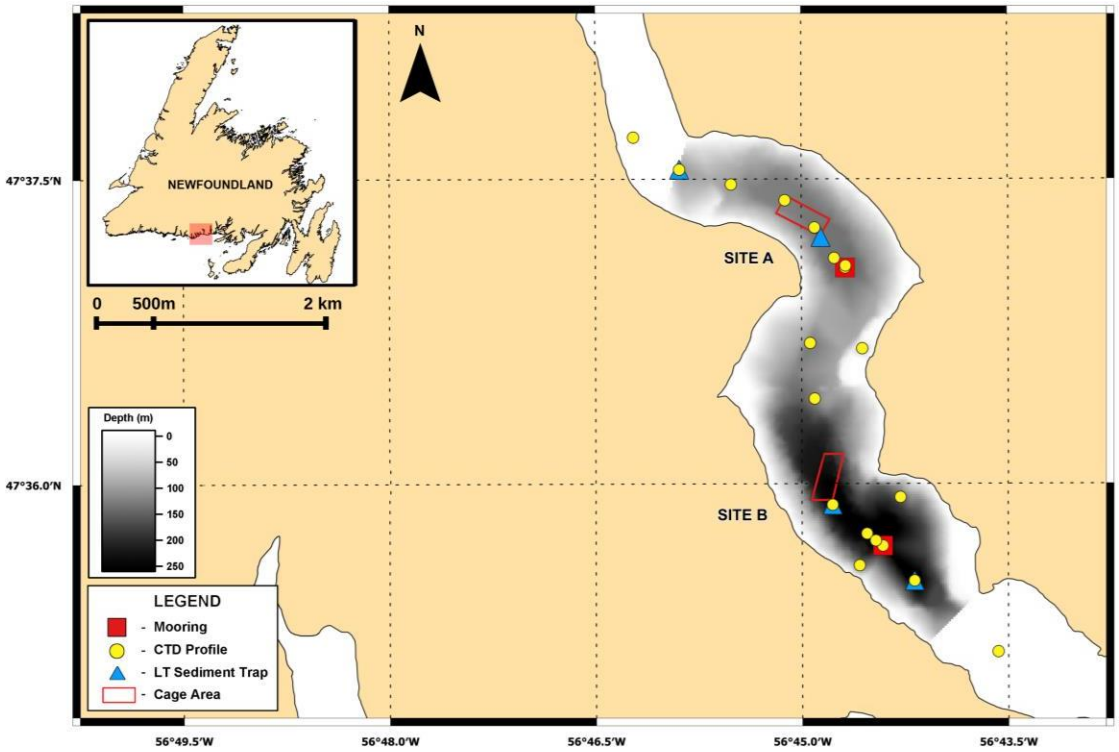

Figure 1: Map of the area showing Site A and Site B and the location of the measurements.

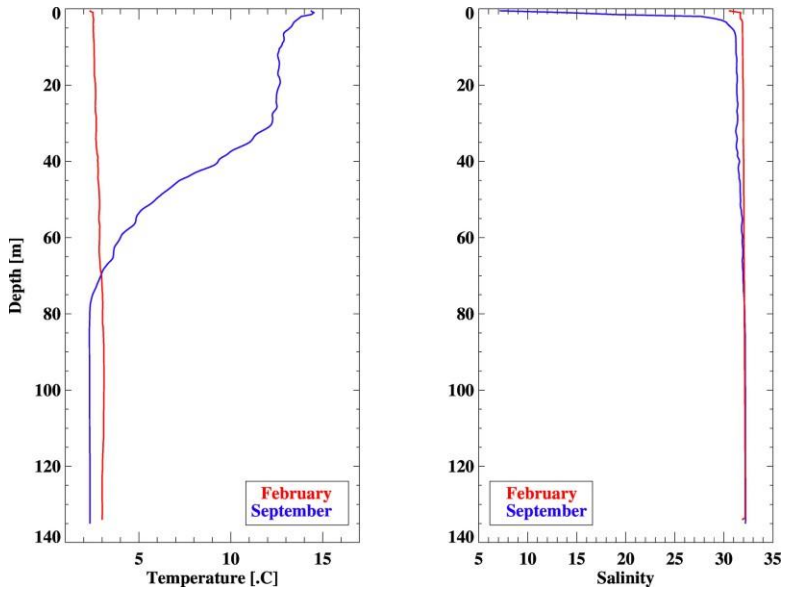

Figure 2: Profile of temperature (left panel) and salinity (right panel) measured near Site A in February and September 2022.

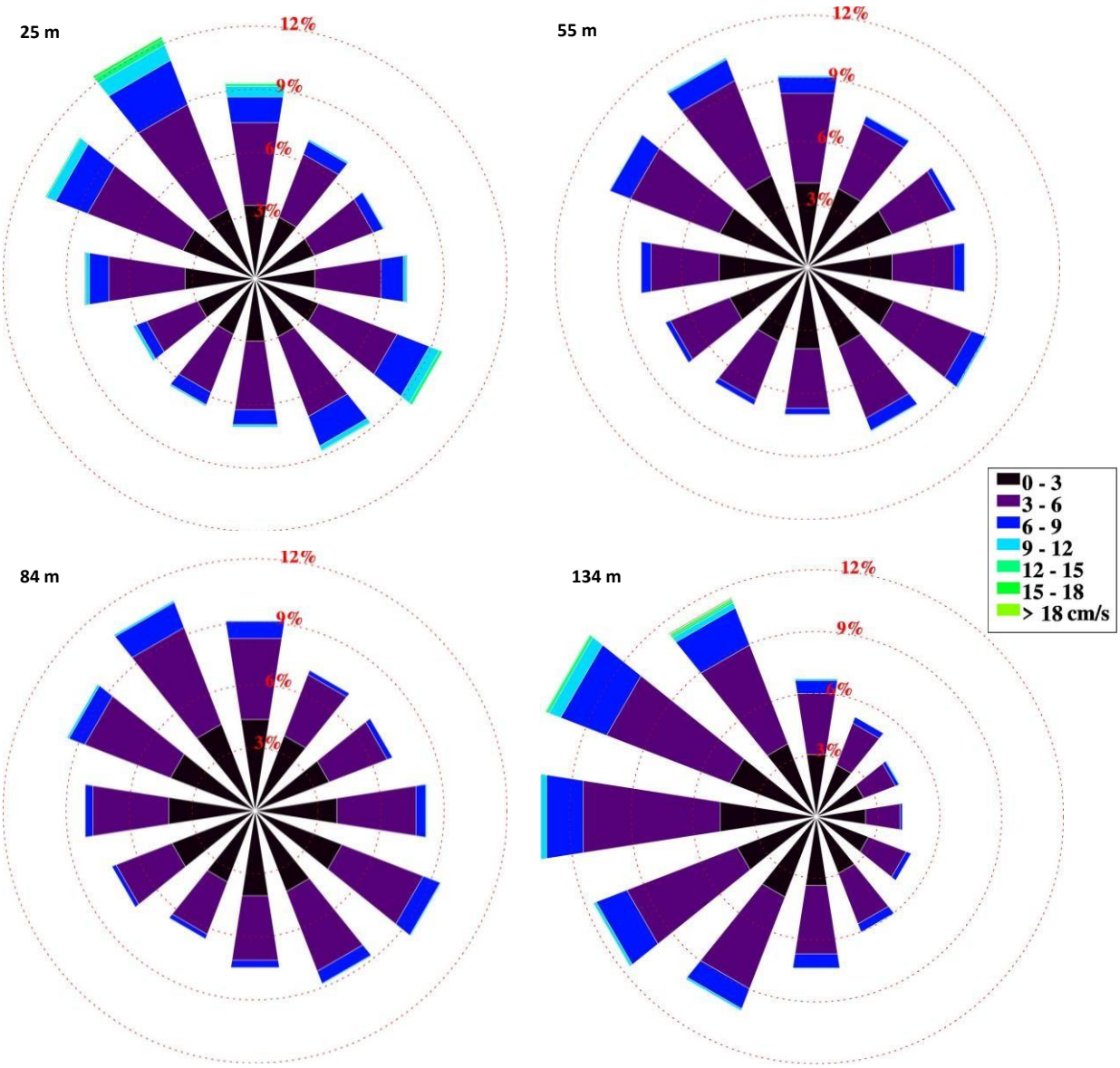

Figure 3: Current rose (rotated to follow the main direction of the channel) showing the distribution of current magnitude and direction measured at selected depths (25, 54, 84, 134 m) for Site A representing the entire period of measurement. The sticks represent the direction where the currents are heading.

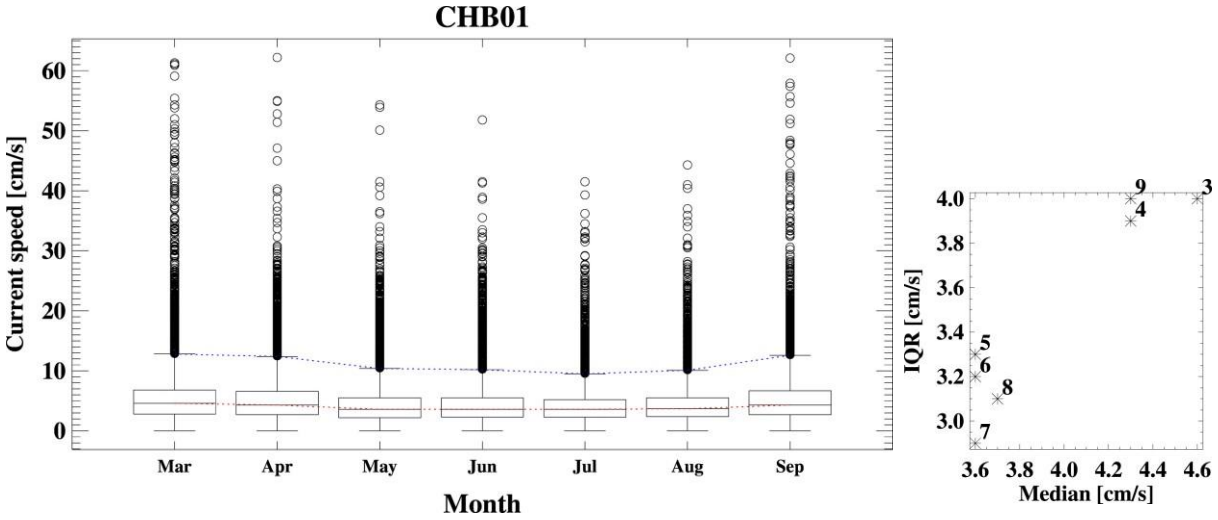

Figure 4: Boxplot of monthly current speed (showing the lower whisker limit, the first quartile, the median, the third quartile, the upper whisker limit, and the outlier data) in the near surface layer (upper 30 m) for Site A (left panel) and scatterplot of monthly values of median speed and interquartile range, IQR (right panel).

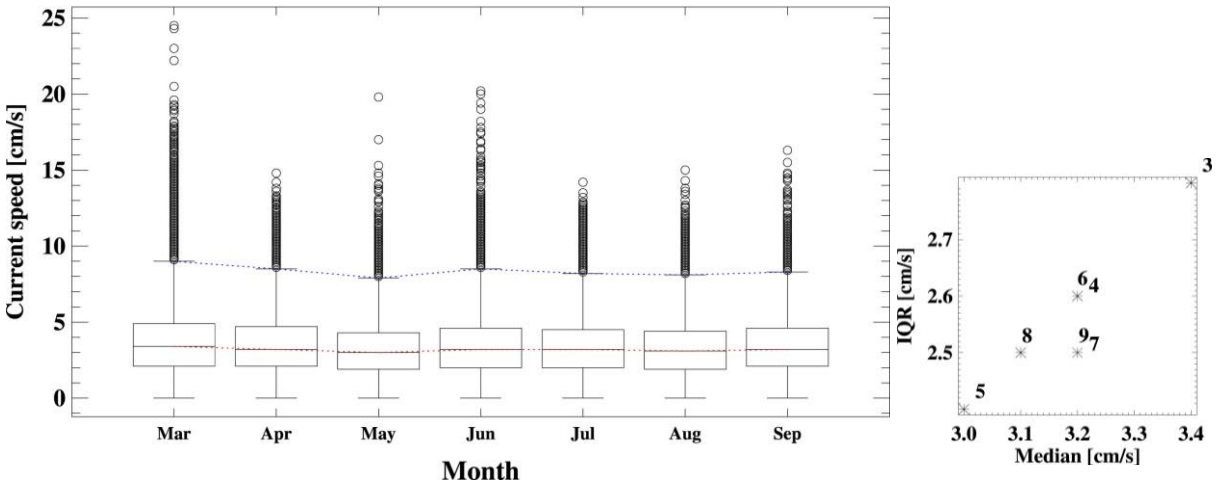

Figure 5: Boxplot of monthly current speed (showing the lower whisker limit, the first quartile, the median, the third quartile, the upper whisker limit, and the outlier data) in the near seafloor layer (lower 30 m) for Site A (left panel) and scatterplot of monthly values of median speed and interquartile range, IQR (right panel).

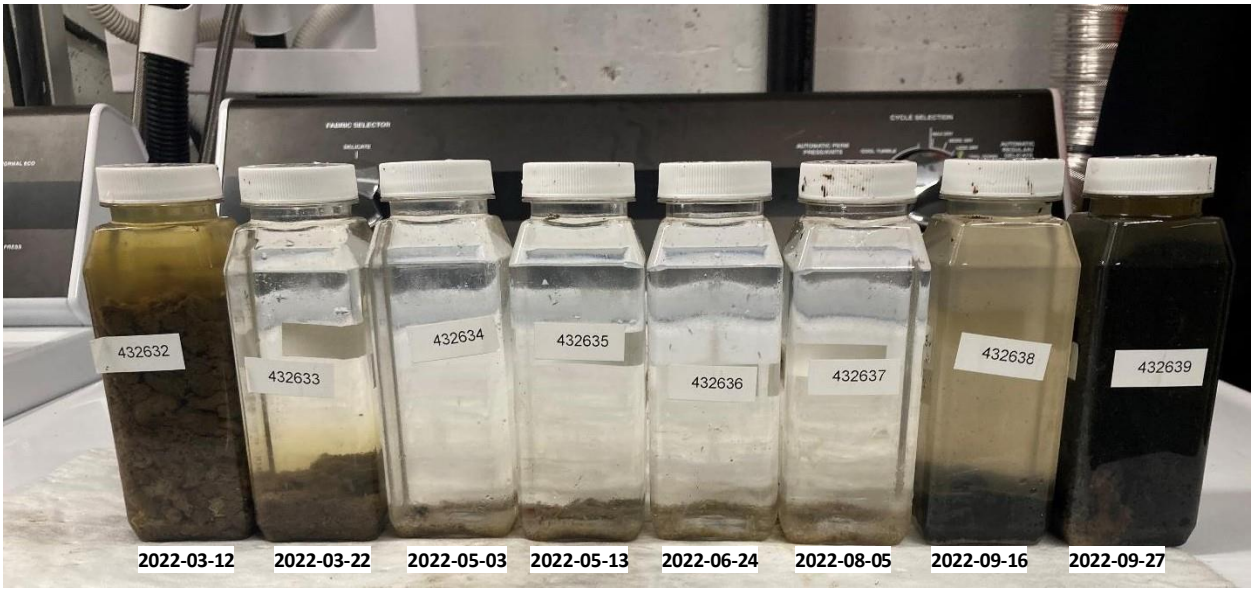

Figure 6: Sediment collection at the edge of the cage array at Site A. Dates correspond to the schedule defined in Table 1.

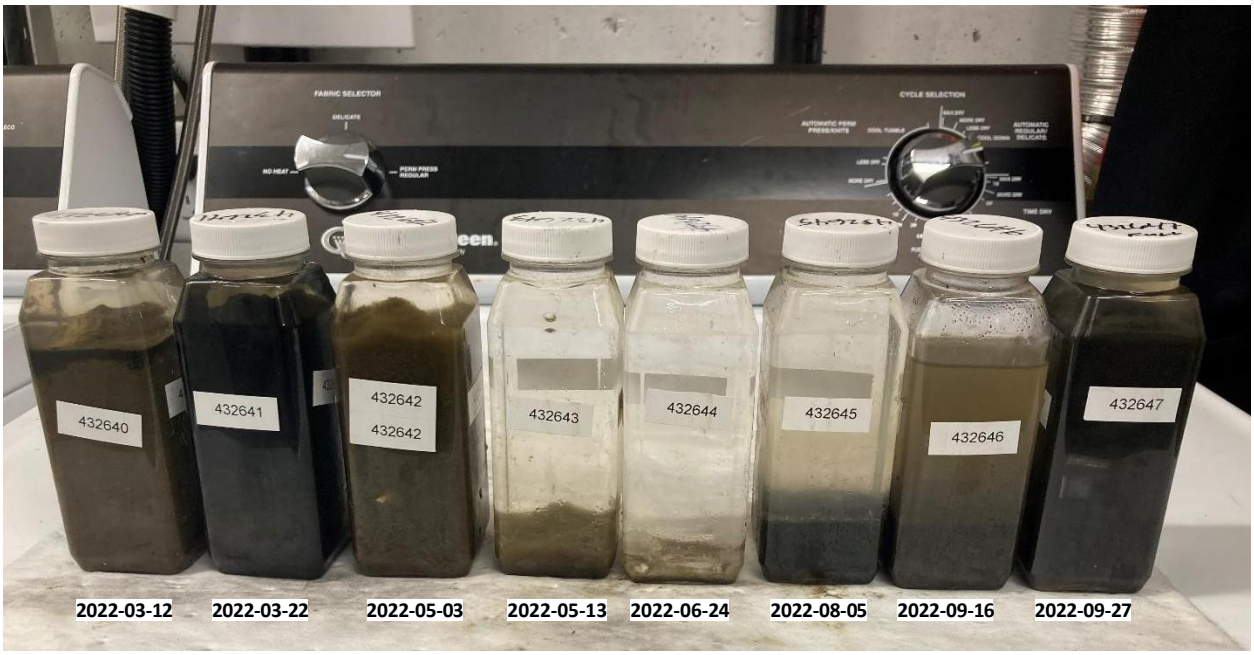

Figure 7: Sediment collection at the edge of the cage array at Site B. Dates correspond to the collection schedule defined in Table 1.

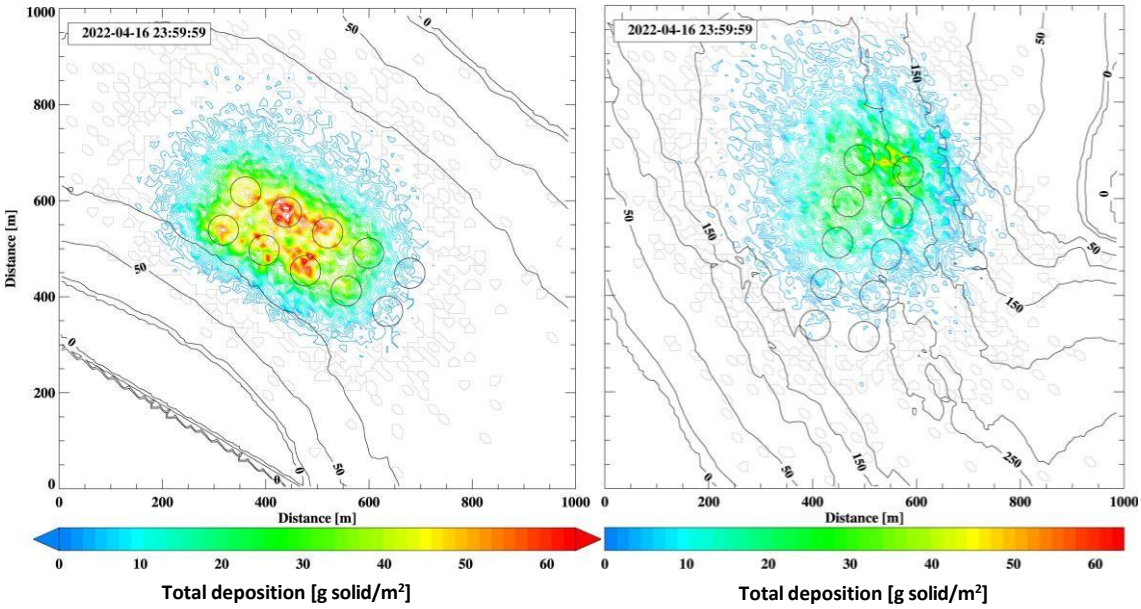

Figure 8: Map of total deposition [g solid/m^2] for the week of 10-16 Apr 2022 for Site A (left panel) and Site B (right panel) as computed using a 10 m x 10 m resolution grid. Also presented on the maps (polygons in light grey) are locations away from the cage area where deposition is relatively small (< 0.1 g solid/m2).

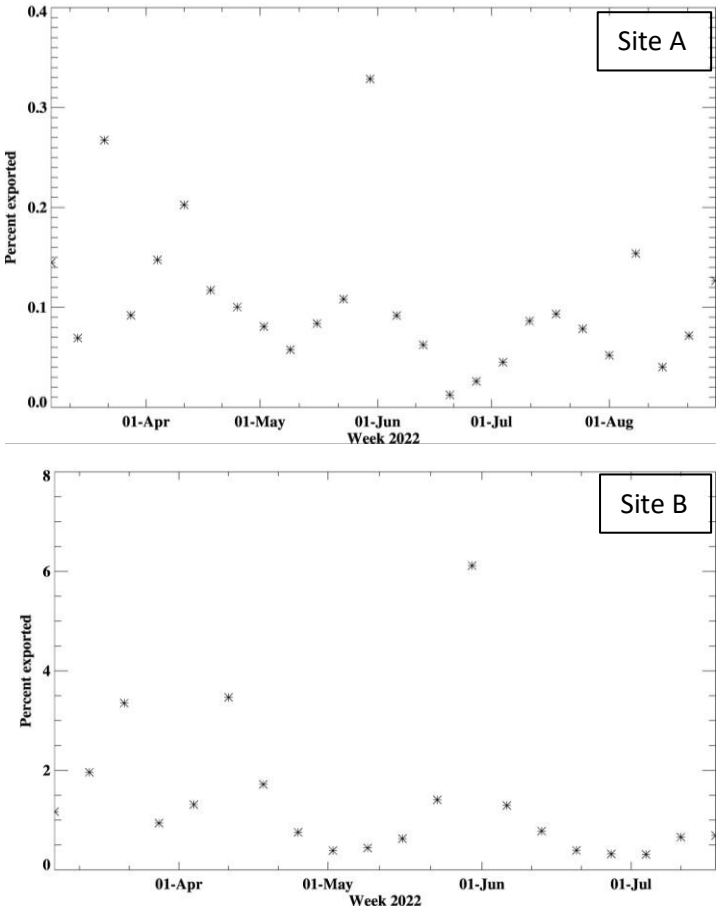

Figure 9: Weekly percentage of deposition exported outside of the 1000-m domain around the site related to the expected total amount of waste deposition when no resuspension is considered. Upper and lower panel illustrate the percentage at Site A and Site B, respectively.

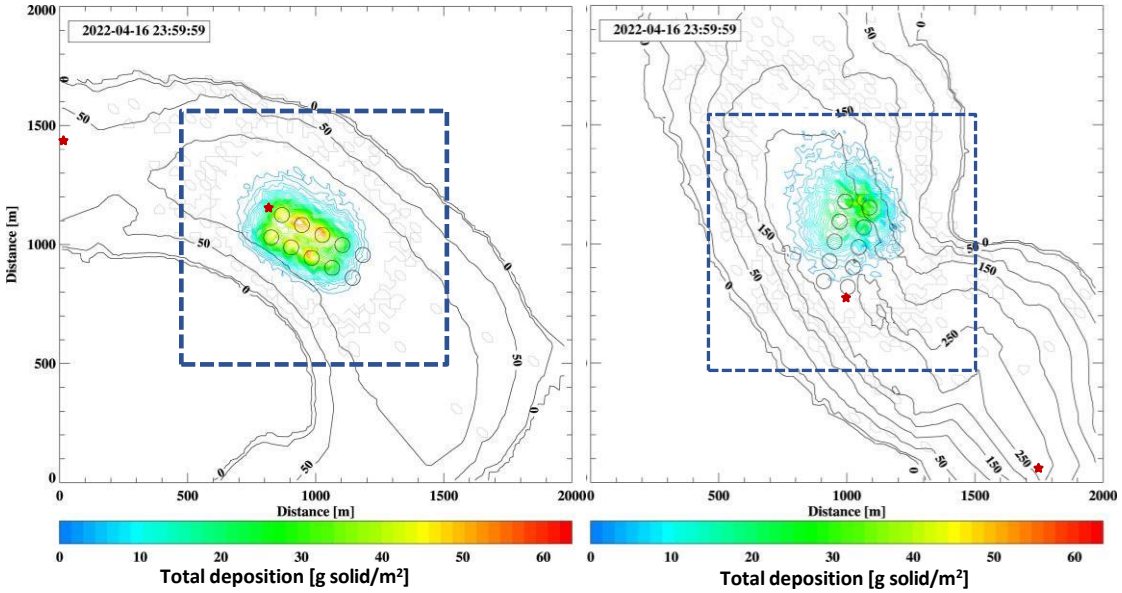

Figure 10: Map of total deposition [g solid/m^2] for the week of 10-16 April 2022 for Site A (left panel) and Site B (right panel) computed using a 20 m x 20 m resolution grid. Area delimited by blue dashed line represents the region of study which corresponds to the 10 m x 10 m grid resolution. Red star marks are the location of the programmable sediment trap (0 m at the cage edge and 1000 m away from the site). Also presented on the maps (polygons in light grey) are locations away from the cage area where deposition is relatively small (< 0.1 g solid/m2).

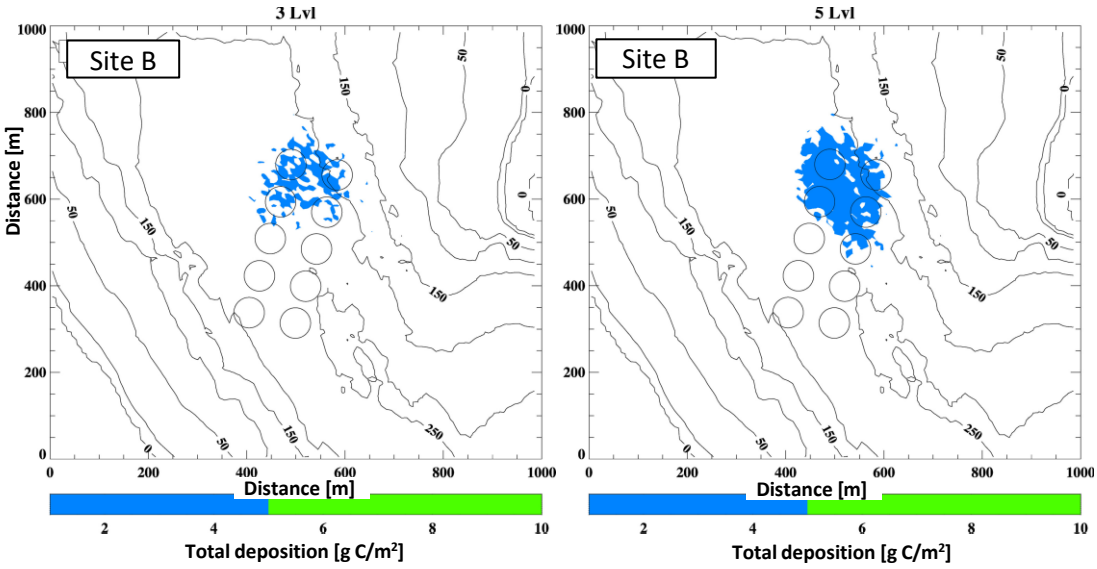

Figure 11: Map of Site B site showing the estimated footprints of BOD matter for the week of 10-16 April 2022. Note that the color bar refers to the ~1-5 and 5-10 g C/m2/d as required by the AAR with the result not showing any flux above 5 g C/m2/d . Left panel is computed using three levels of current timeseries and right panel using five levels of current timeseries.

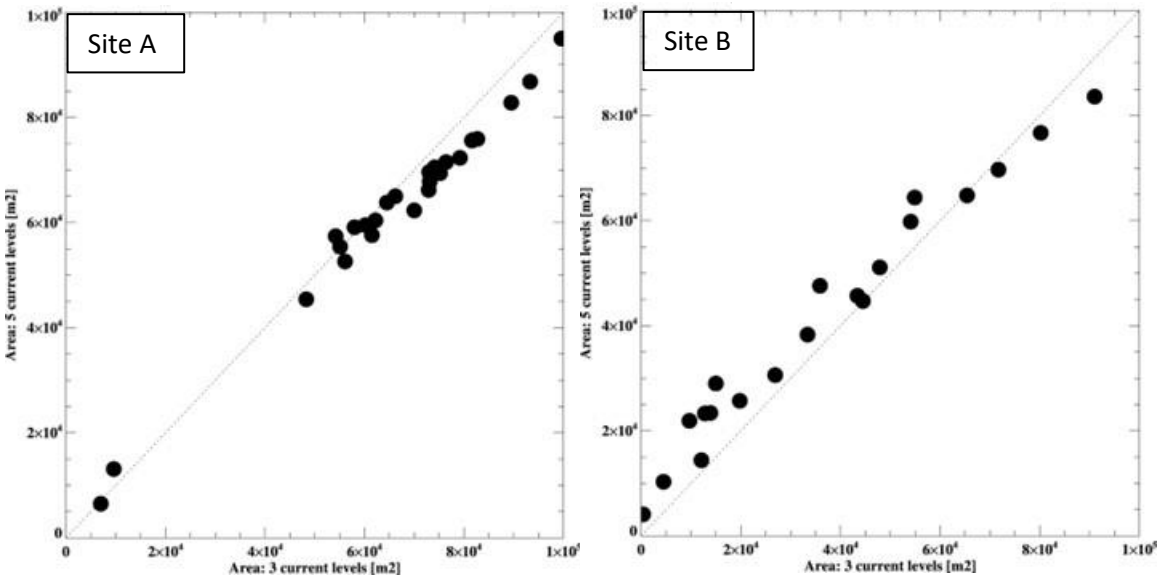

Figure 12: Scatterplot showing the area which corresponds to the ~1-5 g C/m²/d footprint for three-level currents vs. five-level currents. Left panel is for Site A and right panel for Site B.

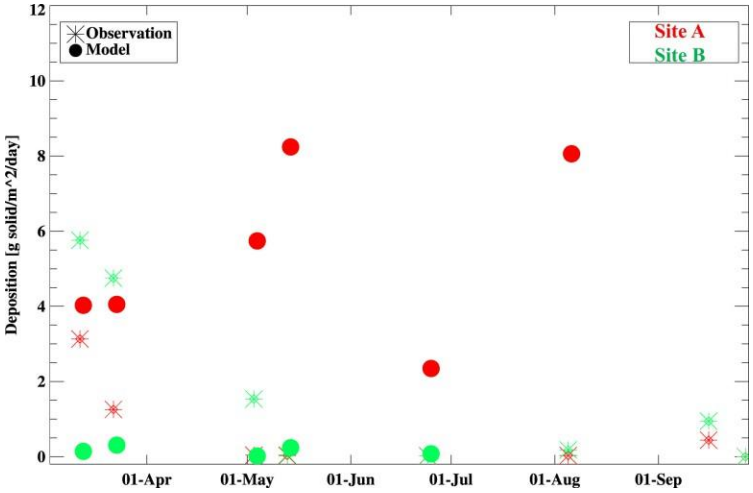

Figure 13: Comparison of rate of deposition between sediment trap collection and modelled result.

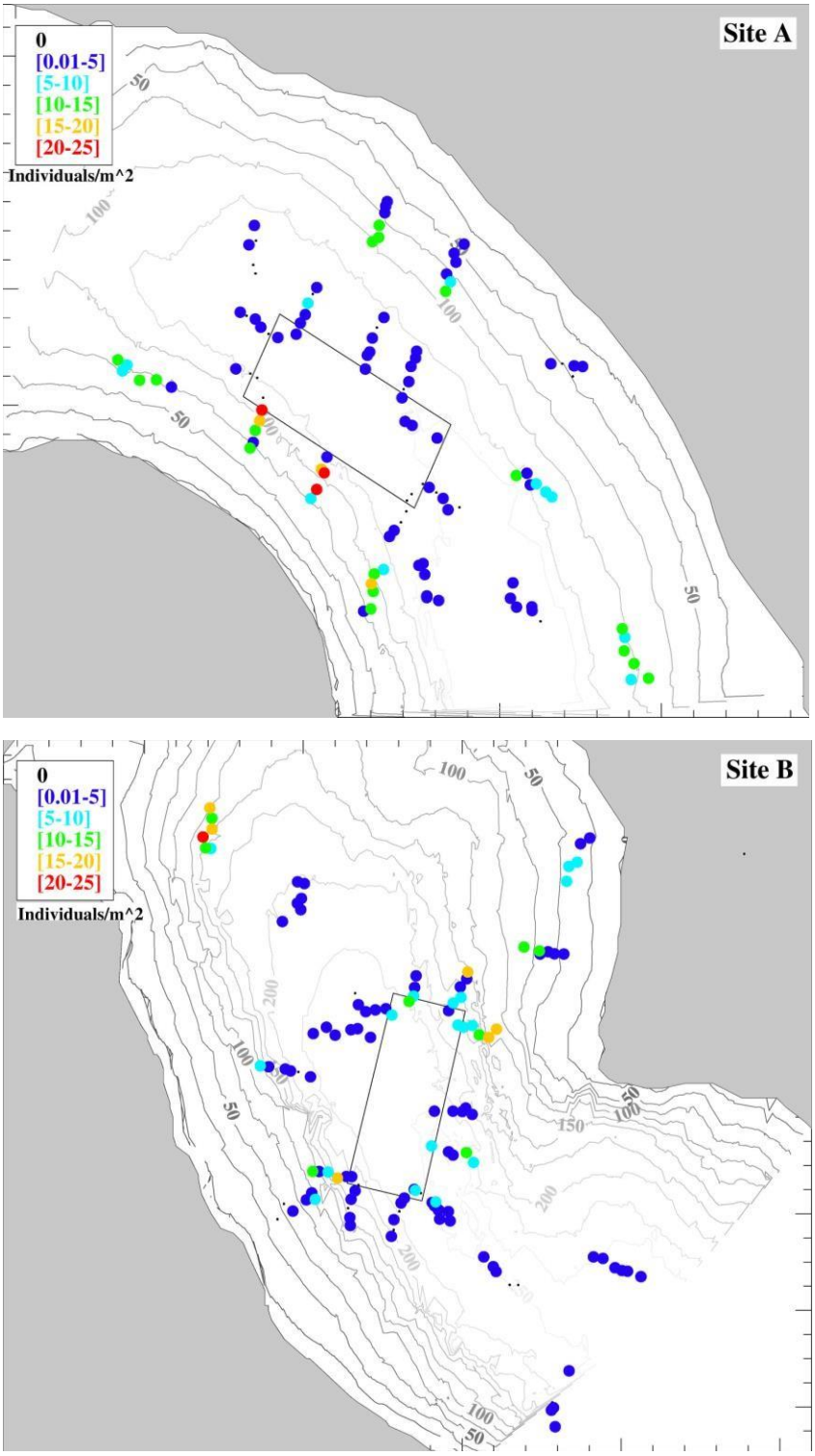

Figure 14: Map showing species abundance (number of observed individuals per m^2 during survey without any distinction among species). Upper panel shows abundance around Site A, lower panel abundance around Site B site. Survey was carried out in Oct. 2022. Small dots in black identify location where no species was observed.

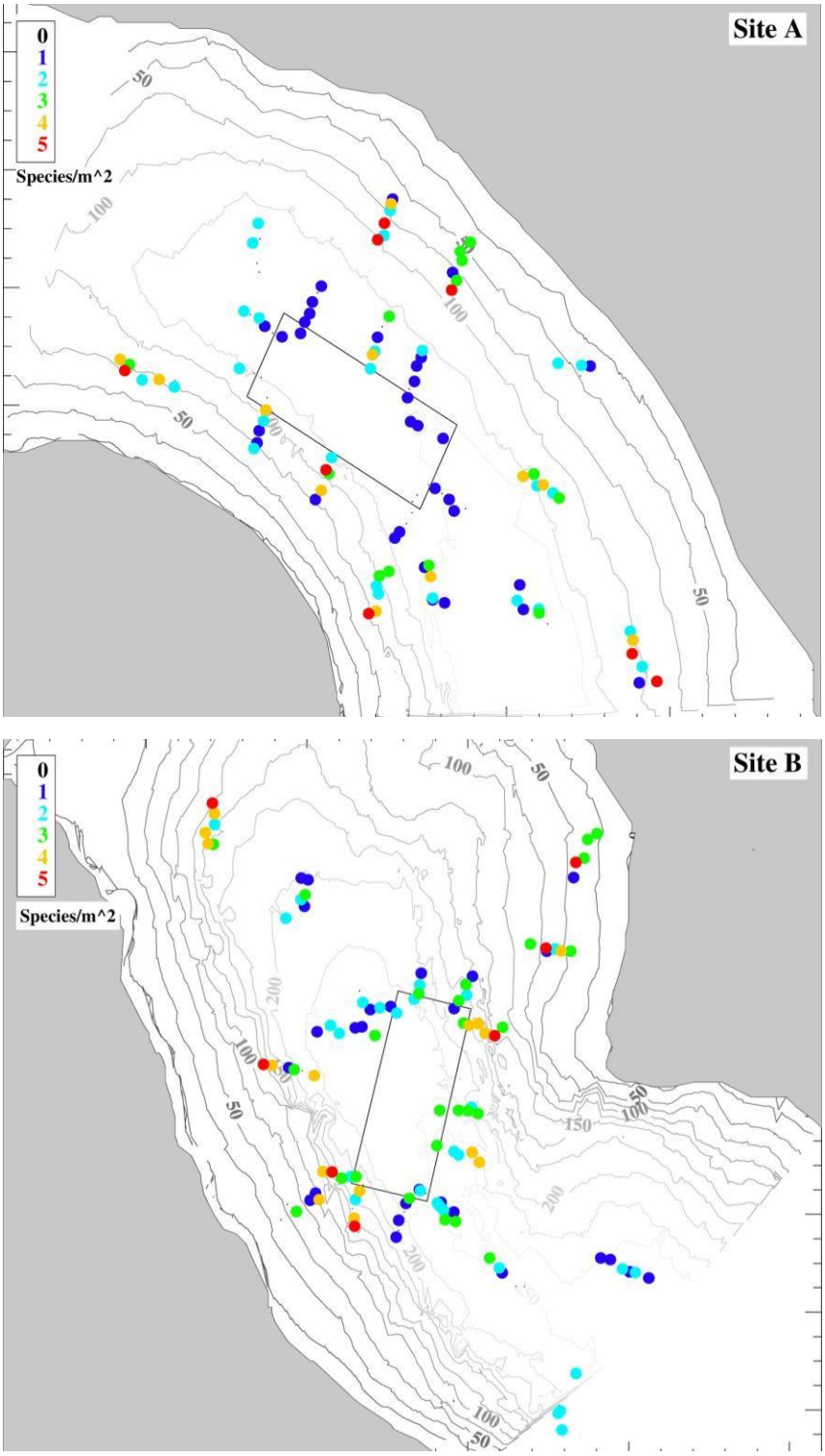

Figure 15: Map showing species diversity (number different species observed at each station). Upper panel shows diversity around Site A, lower panel diversity around Site B. Survey was carried out in Oct 2022. Small dots in black identify location where no species was observed.

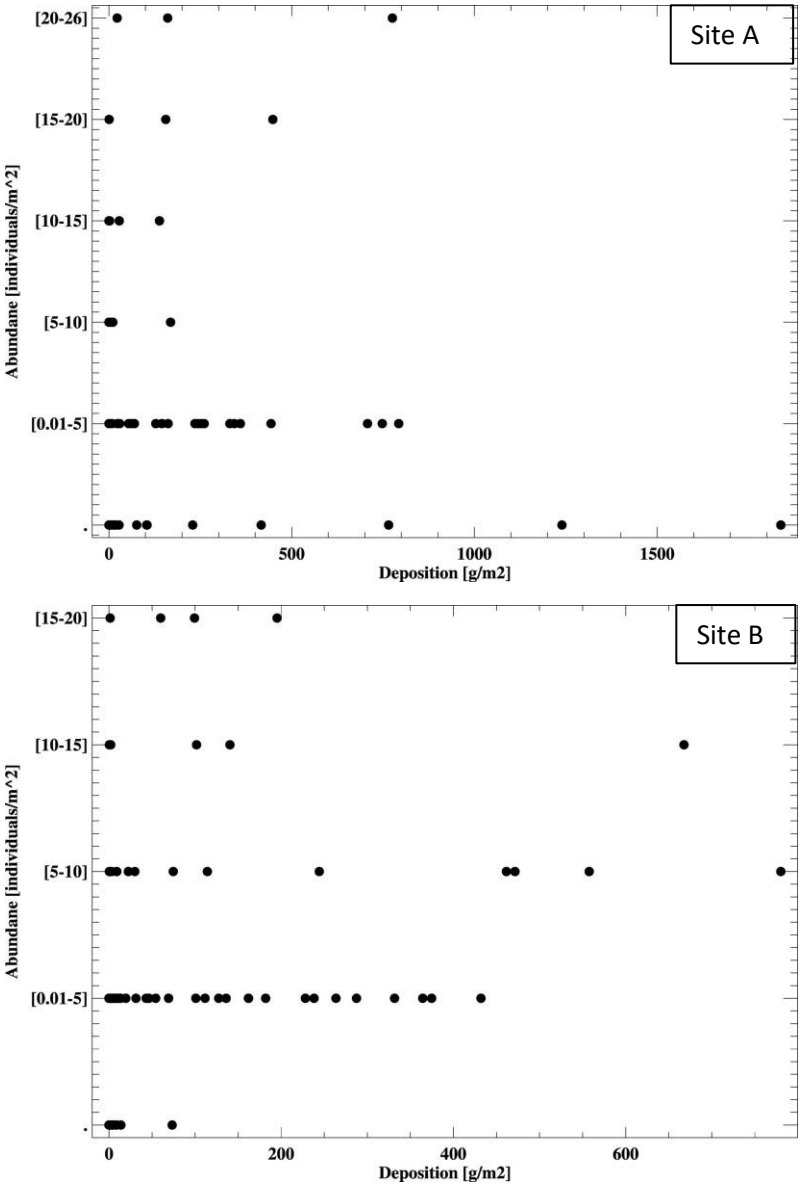

Figure 16: Abundance of individuals per transect as a function of the total deposition computed by DEPOMOD.

APPENDIX

Appendix 1: Currents at Site B

Appendix 2: Percentage of deposition exported outside of the 1000-m domain for model run with resuspension.

Appendix 1

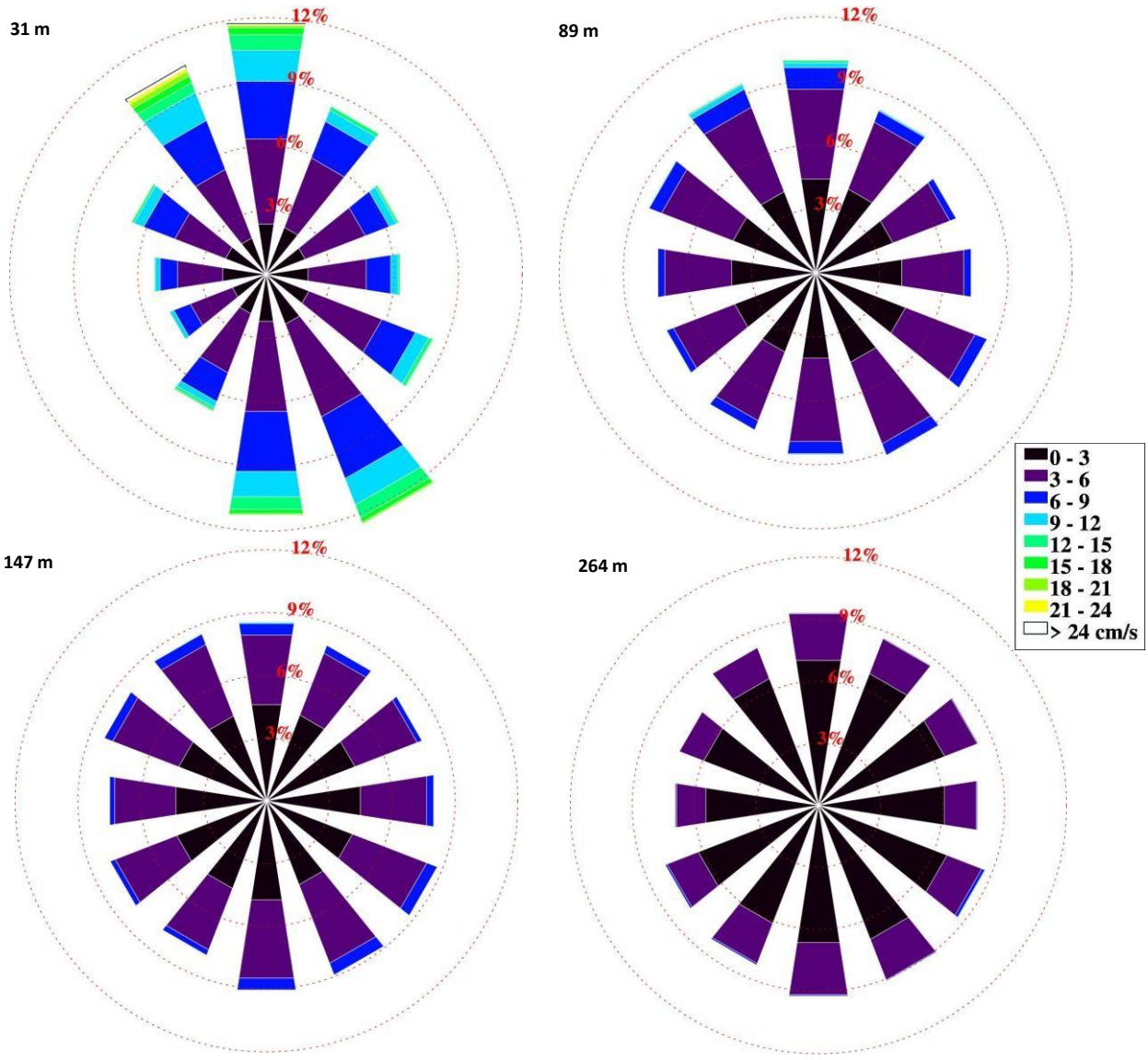

Figure 17: Current rose (rotated to follow the main direction of the channel) showing the distribution of current magnitude and direction measured at selected depths (31, 89, 147, 264 m) for Site B representing the entire period of measurement. The sticks represent the direction where the currents are heading.

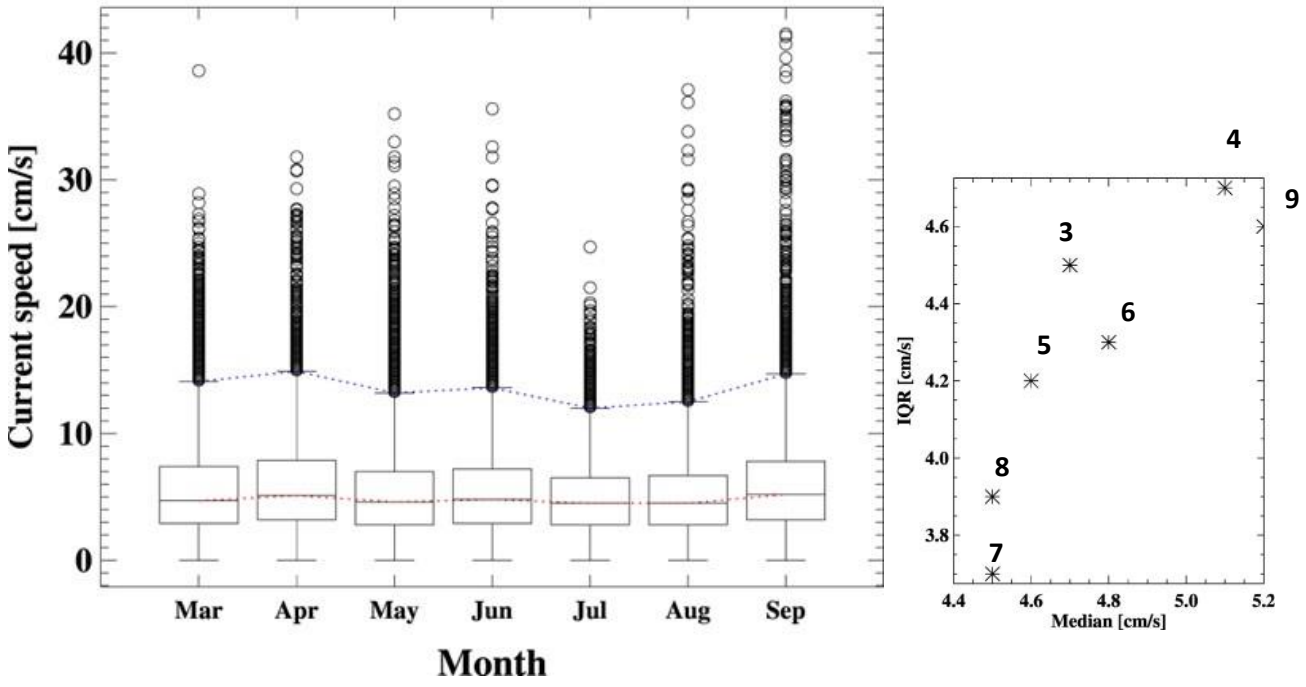

Figure 18: Boxplot of monthly current speed in the surface layer (20-40 m) for Site B (left panel) and scatterplot of monthly values of median speed and interquartile range, IQR (right panel).

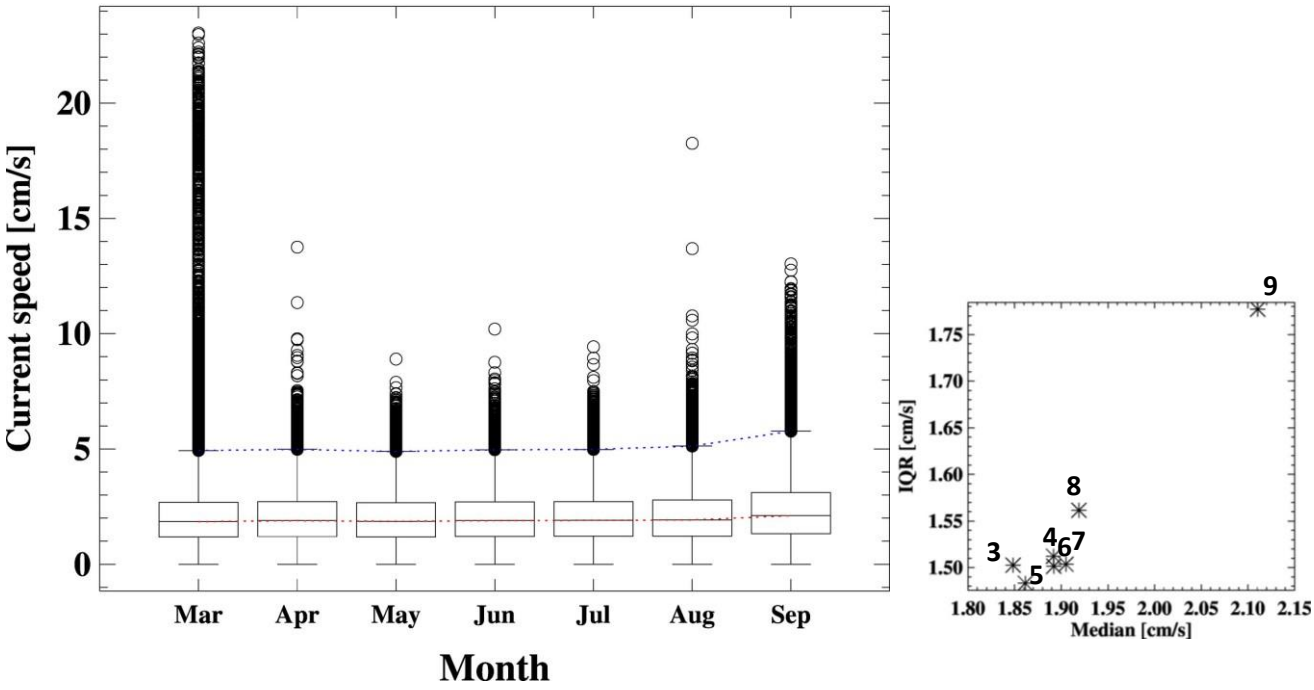

Figure 19: Boxplot of monthly current speed in the near seafloor layer (257-264 m) for Site B (left panel) and scatterplot of monthly values of median speed and interquartile range, IQR (right panel).

Appendix 2

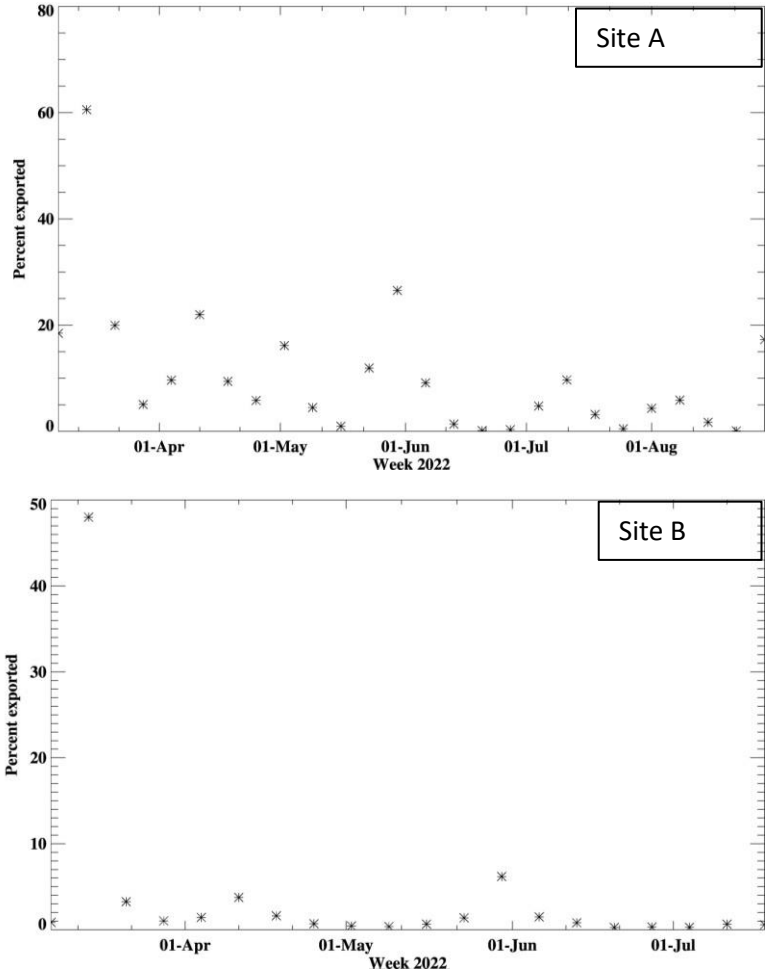

Figure 20: Percentage of deposition exported outside of the 1000-m domain around the site related to the expected total amount of waste deposition when resuspension is activated in the model configuration. Upper (lower) panel illustrates the percentage at Site A (Site B).